

**NASA TECHNICAL
MEMORANDUM**

NASA TM X-53719

March 25, 1968

NASA TM X-53719

**AN EXPERIMENTAL STUDY OF PULSATING
FLOW OF INCOMPRESSIBLE VISCOUS FLUIDS IN
RIGID PIPES IN THE INTERMEDIATE DAMPING RANGE**

By F. R. Goldschmied
Astrionics Laboratory


(NASA-TM-X-53719) AN EXPERIMENTAL STUDY OF
PULSATING FLOW OF INCOMPRESSIBLE VISCOUS
FLUIDS IN RIGID PIPES IN THE INTERMEDIATE
DAMPING RANGE (NASA) 58 p Avail: NTIS

N87-70409

Unclas
00/34 0071542

NASA

*George C. Marshall
Space Flight Center,
Huntsville, Alabama*

FF No. 602(A)		(ACCESSION NUMBER)	(THRU)
	60	(PAGES)	none
		(NASA CR OR TMX OR AD NUMBER)	(CATEGORY)
	AVAILABLE TO NASA OFFICES AND NASA RESEARCH CENTERS ONLY		



NASA-GEORGE C. MARSHALL SPACE FLIGHT CENTER

TECHNICAL MEMORANDUM X-53719

AN EXPERIMENTAL STUDY OF PULSATING FLOW OF
INCOMPRESSIBLE VISCOUS FLUIDS IN RIGID PIPES
IN THE INTERMEDIATE DAMPING RANGE

By

F. R. Goldschmied*

* Prepared under Grant No. NGR 45-003-041 by the Fluid Control Systems Laboratory, University of Utah, Salt Lake City, Utah.

ASTRIONICS LABORATORY
RESEARCH AND DEVELOPMENT OPERATIONS

AN EXPERIMENTAL STUDY OF PULSATING FLOW OF
INCOMPRESSIBLE VISCOUS FLUIDS IN RIGID PIPES
IN THE INTERMEDIATE DAMPING RANGE

By

F. R. Goldschmied*

George C. Marshall Space Flight Center
Huntsville, Alabama

ABSTRACT

This report presents an experimental verification of Womersley's method for the calculation of instantaneous flow rate in a pulsating incompressible flow from the measured instantaneous longitudinal pressure gradient in rigid pipes. The method of computation is applicable to any complex flow pulse. The experimental flow generation was based on fluidic and peristaltic pumps producing a variety of pulsatile and oscillatory flows having finite mean flow rates. Digital computer calculations of instantaneous flow rates were in good agreement with measured data. The instantaneous phase angle between pressure and flow was also investigated and was found to be a function of the pipe Stokes number.

* Prepared under Grant No. NGR 45-003-041 by the Fluid Control Systems Laboratory, University of Utah, Salt Lake City, Utah.

TABLE OF CONTENTS

	Page
INTRODUCTION	1
THEORY.	2
EXPERIMENTAL APPARATUS PROCEDURE	6
EXPERIMENTAL AND COMPUTED RESULTS.	7
DISCUSSION	9
CONCLUSIONS	11
APPENDIX - FORTRAN COMPUTER PROGRAM.	38
REFERENCES	46

LIST OF ILLUSTRATIONS

Figure	Title	Page
1.	Schematic of Apparatus	12
2.	Fluidic Pump with Cover Removed	13
3.	Peristaltic Pump	13
4.	Run 1. Measured Pressure Gradient, Measured Flow Rate, and Computed Flow Rate using Peristaltic Pump. Stokes Number 870; Effective Reynolds Number 1566; Pulse Frequency 1.27 Hz	14
5.	Run 2. Measured Pressure Gradient, Measured Flow Rate, and Computed Flow Rate Using Peristaltic Heart Pump. Stokes Number 1089; Effective Reynolds Number 2033; Pulse Frequency 1.59 Hz	15
6.	Run 3. Measured Pressure Gradient, Measured Flow Rate, and Computed Flow Rate Using Peristaltic Heart Pump. Stokes Number 1347; Effective Reynolds Number 2538; Pulse Frequency 1.96 Hz	16
7.	Run 4. Measured Pressure Gradient, Measured Flow Rate, and Computed Flow Rate Using Peristaltic Heart Pump. Stokes Number 1597; Effective Reynolds Number 2819; Pulse Frequency 2.33 Hz	17
8.	Run 5. Measured Pressure Gradient, Measured Flow Rate, and Computed Flow Rate Using Peristaltic Heart Pump. Stokes Number 2078; Effective Reynolds Number 4143; Pulse Frequency 3.03 Hz.	18
9.	Run 6. Measured Pressure Gradient, Measured Flow Rate, and Computed Flow Rate Using Fluidic Heart Pump. Stokes Number 687; Effective Reynolds Number 8938; Pulse Frequency 1.00 Hz	19

LIST OF ILLUSTRATIONS (Continued)

10.	Run 7. Measured Pressure Gradient, Measured Flow Rate, and Computed Flow Rate Using Fluidic Heart Pump. Stokes Number 758; Effective Reynolds Number 2787; Pulse Frequency 1.09 Hz	20
11.	Run 8. Measured Pressure Gradient, Measured Pressure, Measured Flow Rate, and Computed Flow Rate Using Fluidic Heart Pump. Stokes Number 803; Effective Reynolds Number 10 826; Pulse Frequency 1.22 Hz	21
12.	Run 9. Measured Pressure Gradient, Measured Flow Rate, and Computed Flow Rate Using Fluidic Heart Pump. Stokes Number 837; Effective Reynolds Number 9445; Pulse Frequency 1.19 Hz	22
13.	Run 10. Measured Pressure Gradient, Measured Flow Rate, and Computed Flow Rate Using Fluidic Heart Pump. Stokes Number 872; Effective Reynolds Number 5535; Pulse Frequency 1.25 Hz	23
14.	Run 11. Measured Pressure Gradient, Measured Flow Rate, and Computed Flow Rate Using Fluidic Heart Pump. Stokes Number 902; Effective Reynolds Number 2324; Pulse Frequency 1.32 Hz.	24
15.	Run 12. Measured Pressure Gradient, Measured Flow Rate, and Computed Flow Rate Using Fluidic Heart Pump. Stokes Number 1009; Effective Reynolds Number 10 135; Pulse Frequency 1.43 Hz.	25
16.	Run 13. Measured Pressure Gradient, Measured Flow Rate, and Computed Flow Rate Using Fluidic Heart Pump. Stokes Number 1039; Effective Reynolds Number 2107; Pulse Frequency 1.52 Hz.	26

LIST OF ILLUSTRATIONS (Continued)

Figure	Title	Page
17.	Run 14. Measured Pressure Gradient, Measured Flow Rate, and Computed Flow Rate Using Fluidic Heart Pump. Stokes Number 1353; Effective Reynolds Number 2798; Pulse Frequency 1.89 Hz	27
18.	Run 15. Measured Pressure Gradient, Measured Flow Rate, and Computed Flow Rate Using Fluidic Heart Pump. Stokes Number 1648; Effective Reynolds Number 2051; Pulse Frequency 2.44 Hz	28
19.	Run 16. Measured Pressure Gradient, Measured Flow Rate, and Computed Flow Rate Using Fluidic Heart Pump. Stokes Number 1724; Effective Reynolds Number 3842; Pulse Frequency 2.44 Hz	29
20.	Run 17. Measured Pressure Gradient, Measured Flow Rate, and Computed Flow Rate Using Fluidic Heart Pump. Stokes Number 1782; Effective Reynolds Number 1923; Pulse Frequency 2.63 Hz	30
21.	Run 18. Measured Pressure Gradient, Measured Flow Rate, and Computed Flow Rate Using Fluidic Heart Pump. Stokes Number 2050; Effective Reynolds Number 2070; Pulse Frequency 3.20 Hz	31
22.	Run 19. Measured Pressure Gradient, Measured Flow Rate, and Computed Flow Rate Using Fluidic Heart Pump. Stokes Number 2112; Effective Reynolds Number 2345; Pulse Frequency 3.13 Hz	32
23.	Run 20. Measured Pressure Gradient, Measured Flow Rate, and Computed Flow Rate Using Linford Experimental Data. Stokes Number 77; Pulse Frequency 0.214 Hz	33

LIST OF ILLUSTRATIONS (Concluded)

Figure	Title	Page
24.	Run 21. Measured Pressure Gradient, Measured Flow Rate, and Computed Flow Rate Using Linford Experimental Data. Stokes Number 778; Pulse Frequency 0.169 Hz	34
25.	Run 22. Measured Pressure Gradient, Measured Flow Rate, and Computed Flow Rate Using Linford Experimental Data. Stokes Number 1774; Pulse Frequency 0.309 Hz	35
26.	Phase Shift Angle against Stokes Number for Sinusoidal Oscillatory Pipe Flow	36
27.	Critical Reynolds Number against Velocity Amplitude Ratio for Various Values of Stokes Number	37

DEFINITION OF SYMBOLS

A_0	mean of pressure gradient pulse, N/m^2
A, B	Fourier coefficients of pressure gradient pulse
C	constant of differential equation
D	tube diameter, m
f	pulse frequency, Hz
g	gravity constant, $N \cdot m^2 \text{ kg}^{-2}$
J_0, J_1	Bessel functions of first kind of order zero and one, respectively
k	$(\alpha M_0) / (2M_1)$
K	pressure gradient peak
L	length, m
M	modulus of pressure gradient
\dot{M}	mass flow rate, kg/s
M_0, M_1	moduli of J_0, J_1 , respectively
M^1	$\frac{1}{k} [\sin^2 \sigma + (k - \cos \sigma)^2]^{\frac{1}{2}}$
n	refers to nth harmonic
N	number of Fourier harmonics
P	pressure, N/m^2
P_0	static pressure, N/m^2

DEFINITION OF SYMBOLS (Continued)

Q	total flow rate, m^3/s
Q_n	alternating flow component, m^3/s
Q_0	steady (mean) flow component, m^3/s
\bar{R}	gas constant, $\text{J} \cdot \text{K}^{-1} \text{mol}^{-1}$
R_{eo}	effective Reynolds number, $\frac{4Q_0\rho}{\pi D\mu}$
R_e	Reynolds number, $\frac{vD\rho}{\mu}$
S	Stokes number, $\frac{D^2\omega}{\nu}$
t	time, s
T	temperature, $^{\circ}\text{K}$
u	velocity coefficient, dependent upon radial position
v	velocity, m/s
V	volume, m^3
\dot{W}	weight flow rate, $\dot{\text{Mg}}$
x	axial distance, m
y	dimensionless radial coordinate, r/R
α	characteristic parameter, $R\sqrt{\frac{\omega}{\nu}}$
ρ	mass density, kg/m^3
δ	$135^{\circ} - \theta_1 + \theta_0$

DEFINITION OF SYMBOLS (Concluded)

ϵ	phase angle complement between flow and pressure gradient, $\arctan (\sin \delta / [k - \cos \delta])$
θ_1, θ_0	phase angles of J_0, J_1 , respectively, rad
μ	dynamic viscosity, $\text{N}\cdot\text{s}/\text{m}^2$
ν	kinematic viscosity, m^2/s
ω	angular frequency, $2\pi f$
γ	ρg , weight density
ϕ	phase angle of pressure gradient pulse, rad.

AN EXPERIMENTAL STUDY OF PULSATING FLOW OF INCOMPRESSIBLE VISCOUS FLUIDS IN RIGID PIPES IN THE INTERMEDIATE DAMPING RANGE

SUMMARY

This report presents an experimental verification of Womersley's method for the calculation of instantaneous flow rate in a pulsating incompressible flow from the measured instantaneous longitudinal pressure gradient in rigid pipes. The method of computation is applicable to any complex flow pulse. The experimental flow generation was based on fluidic and peristaltic pumps producing a variety of pulsatile and oscillatory flows having finite mean flow rates. Digital computer calculations of instantaneous flow rates were in good agreement with measured data. The instantaneous phase angle between pressure and flow was also investigated and was found to be a function of the pipe Stokes number.

INTRODUCTION

The study of modern hydraulic control systems demands adequate knowledge of transient viscous flow in pipes and valve components. In particular, it is important to know the instantaneous relationship between pressure and fluid velocity in oscillating or pulsating viscous incompressible pipe flows.

While the topic of steady viscous pipe flow has received attention from numerous experimenters for more than a century, the study of pulsatile viscous pipe flow has been pursued with significant success only since 1928. The application of Reynolds number similarity to steady pipe flow is now classical, but the analogous application of Stokes number similarity to oscillating pipe flow is still not generally known.

The studies of Grace [1] in 1928 involved the equations of motion, velocity profile, and phasing of pulsating flow. Considerable work has followed, and the number of independent studies has increased exponentially to the present.

The cardiovascular system of the body is vividly pulsating in nature. In this respect, much of the pulsatile flow knowledge that exists today has evolved from the study of blood flow. Several individuals have instrumented the arteries of animals in an attempt to gain an understanding of the circulation system. The collaborated works of McDonald [2], a physiologist, and Womersley [3], a mathematician, are particularly noteworthy, serving as a guide for this project.

The work of Womerley in 1955 stands out as a significant analytical approach for the computation of the velocity profile and instantaneous flow rate in pulsating flow. Linford and Ryan [4], among other workers, using a reciprocating piston pulse generator, were successful in 1965 in matching theory with experimentation. The research involved verification of both instantaneous flow rate and the more difficult velocity profile for the case of zero mean flow discharge. This study has had a similar objective dealing only with flow rate but involving a wide variety of pulse shapes having finite mean flow rates. Because of the nonlinearity of the Navier-Stokes equations, the superposition of a steady flow affects the periodic terms.

For two pipe flows of equal L/D ratio at a very small Mach number to be equivalent in both steady and dynamic states, the Reynolds number, the acoustic Reynolds number, and the Stokes number must be equal. This similarity law can be derived from dimensional analysis and was demonstrated for pipe flow by Goldschmied [5]. The Stokes number was shown to have the characteristics of a dynamic damping index and classifies dynamic fluid flow into regimes in regard to dynamic conditions. Three regimes can be identified by the Stokes number. The high-damping regime comprises the range from steady-state flow ($S = 0$) up to $S = 10$. The intermediate-damping regime comprises the Stokes number range from 10 to 1000; most practical applications fall in this region. The low-damping regime comprises the Stokes number range above 1000.

THEORY

Womersley in his analysis of pulsating flow applied a technique which made possible the expression of a complex wave shape in terms of the Fourier series. In so doing, a pressure gradient wave can be expressed as the sum of a mean and a series of sinusoidal components (the harmonics of the series). Womersley solved the Navier-Stokes equation for one-dimensional flow by assuming a sinusoidal pressure gradient. This approach allows the computation of

instantaneous flow rate for any complex pulse on a term-by-term basis, the sum of which being the resultant flow wave. Each element of the sum can be thought of as an individual flow problem in its own right having its own amplitude, frequency, and phase.

Womersley based his original development on the one-dimensional Navier-Stokes equation for laminar pulsatile flow of an incompressible, Newtonian fluid.

$$\frac{\partial v}{\partial t} = - \frac{1}{\rho} \frac{\partial p}{\partial x} + \nu \left(\frac{\partial^2 v}{\partial r^2} + \frac{1}{r} \frac{\partial v}{\partial r} \right) \quad (1)$$

Equation 1, which may be found in Schlichting (6), applies where tangential and radial components of velocity are zero and where the axial velocity component is independent of the axial station. The pressure gradient was assumed to be the following simple harmonic function to facilitate a solution of the above.

$$- \frac{\partial p}{\partial x} = \text{real} \left(K e^{i\omega t} \right) = M \cos(\omega t + \phi) \quad (2)$$

Similarly, flow velocity may be expressed as a harmonic function

$$v = u e^{i\omega t} \quad (3)$$

where u is a function of radial station. Substitution of equations 2 and 3 into equation 1 and insertion of the dimensionless radial coordinate, $y = \frac{r}{R}$, result in a form of Bessel's equation,

$$\frac{\partial^2 u}{\partial y^2} + \frac{1}{y} \frac{\partial u}{\partial y} + i^3 \alpha^2 u = - \frac{KR^2}{\mu} \quad (4)$$

where a nondimensional characteristic parameter, α , proportional to the square root of Stokes number, S , was introduced for convenience.

$$\alpha = \frac{1}{2}\sqrt{S} = R\sqrt{\frac{\omega}{\nu}} \quad (5)$$

Solution of equation 4 may be obtained by utilizing the boundary condition $u = 0$ at $y = 1$ to achieve the following result written in terms of Bessel functions of the first kind of order zero.

$$u = \frac{KR^2}{i\alpha^2\mu} \left[1 - \frac{J_0(i^{3/2}\alpha y)}{J_0(i^{3/2}\alpha)} \right] \quad (6)$$

Upon returning to the original velocity notation, flow rate may be equated to the integral of velocity over the entire cross section of the tube.

$$Q = \int_0^R vr \, dr = \frac{\pi KR^4}{i\alpha^2\mu} \left[1 - \frac{2J_1(i^{3/2}\alpha)}{i^{3/2}\alpha J_0(i^{3/2}\alpha)} \right] e^{i\omega t} \quad (7)$$

Womersley then chose to express the complex Bessel functions in the form of modulus and phase.

$$J_0(i^{3/2}\alpha) = M_0 e^{i\theta_0} \quad (8)$$

$$J_1(i^{3/2}\alpha) = M_1 e^{i\theta_1} \quad (9)$$

Equations 8 and 9, as well as the right hand side of equation 2, may be substituted into equation 7 to yield the following expression.

$$Q = \frac{\pi R^4}{\mu} \frac{M}{\alpha^2} \left[\sin(\omega t - \phi) - \frac{2M_1}{\alpha M_0} \sin(\omega t - \phi - \delta) \right] \quad (10)$$

The following definitions may then be assigned.

$$k = \frac{\alpha M_0}{2M_1} \quad (11)$$

$$M' = \frac{1}{k} \left[\sin^2 \delta + (k - \cos \delta)^2 \right]^{\frac{1}{2}} \quad (12)$$

$$\tan \epsilon = \sin \delta / (k - \cos \delta) \quad (13)$$

Tables of M'/α^2 and ϵ have been compiled by Womersley for values of α from zero to ten and are given as a computational aid in the appendix to this report. Womersley derived asymptotic expressions for M' and ϵ when α is greater than ten or the Stokes number is approaching 1000.

$$M' = 1 - \frac{\sqrt{2}}{\alpha} + \frac{1}{\alpha^2} \quad (14)$$

$$\epsilon = \frac{\sqrt{2}}{\alpha} + \frac{1}{\alpha^2} + \frac{19}{24\sqrt{2}\alpha^3} \quad (15)$$

The asymptotic expressions apply to the "low-damping" flow regime discussed by Goldschmied [5]. For α greater than twenty (Stokes number, $S > 1600$), M' may be equated to one and ϵ may be equated to zero without appreciable loss of accuracy. This corresponds to a "zero-damping" or acoustic regime which is commonly treated by inviscid acoustic theory. Substitution of equations 11, 12, and 13 into equation 10 and the use of the relationships $A = M \cos \phi$ and $B = M \sin \phi$ result in the final form for calculation of time dependent flow rate for the n th harmonic.

$$Q_n = \frac{\pi R^4}{\mu} \frac{M'_n}{\alpha_n^2} \left[(A_n \sin \epsilon_n - B_n \cos \epsilon_n) \cos n\omega t + (A_n \cos \epsilon_n + B_n \sin \epsilon_n) \sin n\omega t \right] \quad (16)$$

The steady, mean flow may be written according to Poiseuille's law.

$$Q_0 = \frac{\pi R^4 A_0}{8\mu} \quad (17)$$

Summing the steady and pulsating flows results in the total instantaneous flow rate — the object of this derivation:

$$\frac{Q}{Q_0} = 1 + \sum_{n=1}^n \frac{Q_n}{Q_0} \quad (18)$$

EXPERIMENTAL APPARATUS AND PROCEDURE

Figure 1 is a schematic representation of the experimental apparatus. The test section consisted of a straight rigid copper tube having a diameter of 1.11 cm (7/16 in.) and approximate length of 6 m (20 ft). Eleven pressure taps were soldered normal to the tube axis at 0.3048 m (1 ft) intervals with a liberal untapped margin of several meters at either end. A variable reluctance dc output pressure transducer was rated at $\pm 3.44 \text{ N/cm}^2$ (5 psi) differential pressure with a frequency response of 1000 Hz. The flow rate instrumentation consisted of an electromagnetic flow meter with a 0.952 cm (3/8 in.) diameter transducer. Frequency response was variable and could be selected by the operator at a maximum of 150 Hz. A calibration of the measured flow pulse was performed using the digital computer for each run by applying the timed volumetric measurement to the mean of the flow pulse.

Water was used exclusively as the fluid medium. The test system was designed to operate as a closed or an open fluid system. As a closed system, constant equal pressure heads could be maintained at both reservoir and receiver. As an open system, it was possible to obtain mean flow measurements through an overflow spill neck in the receiver tank which emptied into a graduated receptacle for timed volumetric measurements.

Two artificial heart pumps, an electric motor-driven heart pump (Fig. 2) and a fluidic compressed air-driven heart pump (Fig. 3), were employed as pulsating flow generators. The construction and operation of both pumps are fully described by Goldschmied, Prakouras, and Nelson [7].

The peristaltic pump functions by pushing the fluid medium through a distensible tubing lying in a circular track under the influence of a pair of rollers which bear on and collapse the distensible tubing as they traverse its length. The approximate maximum flow output and frequency are 49 cm^3 (3 in.^3) per second and 5 Hz, respectively. The latter parameters are variable according to roller pressure and motor speed, but in all cases they produce a near sinusoidal flow pulse.

The fluidic pump was developed at the University of Utah from a design pioneered by the U. S. Army's Harry Diamond Laboratories. The pump is based on a pneumatic fluidic amplifier which alternately fills and evacuates a soft Silastic ventricle within a brass housing. Bicuspid Daggett valves at water intake and discharge ports are features of the pump design. The fluidic pump used during this experiment was limited in frequency to the range of 1 to 3 Hz. Pumping capacity, with equal filling and static heads of 0.3048 m (1 ft) of water, ranged from 24.6 to 115 cm^3 (1.5 to 7 in.^3) per second.

Pressure gradient measurements were taken at pressure taps 1.22 and 1.525 m (4 and 5 ft) apart along the test section to accommodate the convenient measuring range of the pressure transducer. Other spacings were also tried for differential pressure measurements, resulting in no appreciable difference in differential pressure per meter length.

The two pumps were operated over their ranges of performance to obtain variation in the parameters, frequency, mean flow, and wave shape.

Water temperature, a critical parameter affecting viscosity, was monitored frequently during tests. Water pressure heads of 0.3048 m were maintained at both reservoir and receiver tanks.

EXPERIMENTAL AND COMPUTED RESULTS

A summary of the experimental program performed herein is presented in Table I and illustrated graphically in Figures 4 through 25. The results are presented in order of increasing Stokes number, where the frequency is the fundamental pulsating or oscillating frequency. An additional parameter, the effective Reynolds number, is based on the measured mean flow rate, i. e., the average pumping rate.

TABLE I. EXPERIMENTAL PROGRAM

Run No.	Stokes No. , S	Effective Reynolds No. , R_{eo}	Pulse Frequency, f (Hz)	Mean Flow Rate, Q_0 cm ³ /s (gpm)	Figure No.
Peristaltic Pump					
1	870	1556	1.27	15.40 (0.245)	4
2	1089	2033	1.59	20.05 (0.318)	5
3	1347	2538	1.96	25.00 (0.397)	6
4	1597	2819	2.33	27.80 (0.441)	7
5	2078	4143	3.03	40.80 (0.648)	8
Fluidic Pump					
6	687	8939	1.00	88.20 (1.398)	9
7	758	2787	1.09	27.00 (0.429)	10
8	803	10 826	1.22	111.00 (1.765)	11
9	837	9445	1.19	90.70 (1.442)	12
10	872	5535	1.25	53.7 (0.851)	13
11	902	2324	1.32	22.90 (0.364)	14
12	1009	10 135	1.43	97.00 (1.538)	15
13	1039	2107	1.52	20.80 (0.330)	16
14	1353	2798	1.89	26.40 (0.419)	17
15	1648	2051	2.44	22.55 (0.358)	18
16	1724	3842	2.44	36.80 (0.583)	19
17	1782	1923	2.63	19.25 (0.305)	20
18	2050	2070	3.20	21.85 (0.347)	21
19	2112	2345	3.13	23.5 (0.373)	22
Reciprocating Piston (Linford and Ryan)					
20	77	0	0.214	0	23
21	778	0	0.169	0	24
22	1774	0	0.309	0	25

The measured pressure gradient, measured flow rate, and calculated flow rate are depicted over one complete cycle for each test run. The method of Womersley, as described earlier, was utilized in obtaining calculated flow pulses. A digital computer program was compiled in Fortran IV to fit the measured pressure gradient with a Fourier series. Flow rate was then computed on the basis of each harmonic of the series, and the individual solutions were summed to obtain the resultant calculated flow rate depicted on each plot.

The flow wave shapes obtained with the peristaltic pump were irregular to near sinusoidal. Verification of the theoretical method of Womersley was achieved in terms of phase and amplitude. Note that the shapes of the flow pulses are not evident by inspection of the corresponding pressure gradient pulses. High frequency transients occurred throughout pressure gradient measurements. A considerable portion of the gradient pulse is negative even though no flow reversal was either calculated or measured. Most of these comments apply equally as well to experimental test runs obtained using the fluidic pump where a close correlation of theory and experiment was achieved.

Phase angles between pressure gradient and flow pulses are, as before, difficult to assess because of highly fluctuating data. The pressure gradient pulse may, however, be seen to be clearly leading the flow pulse in all cases; thus, fluid inertia has been demonstrated. A pressure pulse is depicted in Figure 11 and may be seen to be similar in shape to the gradient pulse. Mean values corresponding to steady flow conditions have been noted on all figures. Experimental data, collected by Linford and Ryan [4] in an earlier investigation using a reciprocating piston, have been utilized as an additional criterion. Three representative runs, presented graphically in Figures 23, 24, and 25, have yielded the same correspondence of theory and experiment demonstrated by Linford. The experimental data presented here are based on the work of Zumbrunnen [8] at the Fluid Control Systems Laboratory of the University of Utah.

DISCUSSION

Mean Flow Pressure Gradient

Initially, difficulty was encountered during computations in acquiring a correspondence in the mean levels of calculated and measured flow. Investigation revealed a virtually uncorrectable laboratory measuring problem. The magnitude

of the pressure gradient (the mean) necessary to maintain the steady flow component was very small in comparison with the oscillatory components. Test run 13 (Fig. 16), for example, requires a pressure gradient mean of only $0.00628 \text{ (N/cm}^2\text{) m}^{-1}$ (0.0028 psi/ft) to maintain its mean flow of $20.8 \text{ cm}^3/\text{s}$ (0.3295 gpm); whereas the oscillations in pressure gradient were two orders of magnitude greater. In selecting instrumentation scale factors, the mean gradient was unavoidably lost. This problem has been cited by both McDonald [2] and Rudinger [9]. The only alternative was to superimpose the oscillatory components of the pressure gradient, as defined by the harmonics of the Fourier series, onto the measured mean level such that the measured mean level becomes the reference. This analysis has followed such a procedure.

Phase Angle between Pressure Gradient and Flow

The phase angle between pressure gradient and flow may be shown to be a function of the Stokes number alone for sinusoidal oscillations; this relationship, attributed to Womersley, is shown in Figure 26. The experimental points have been obtained from the work of Linford and Ryan [4] and Sarpkaya [10]; in both cases, the flow oscillation was sinusoidal, but with different upper Stokes number limits, i.e., 2350 in the former and 280 in the latter. It has not been possible to show the phase angle for the pulsatile flow of the present experimental program because of the irregular and complex pulse shapes.

Limit of Applicability of Viscous Flow Theory

The present theory is based on the equation for time-dependent incompressible viscous flow. As such, the theory will not be applicable to large Reynolds numbers and Stokes numbers when the flow is turbulent and the damping negligible. The problem is to estimate the practical limit of engineering applicability of the viscous theory in terms of Reynolds number, Stokes number, and amplitude of oscillation or pulsation. While the critical Reynolds number for steady flow is accepted to be approximately 2000, it has been shown by Sarpkaya [10] that for sinusoidally oscillating flow the critical Reynolds number is a function of the Stokes number and of the amplitude ratio. This dependence is presented in Figure 27, reproducing the data of Figure 10 of Reference 10. At each Stokes number, there is a definite maximum for the critical Reynolds number at some value of the amplitude ratio. It is immediately apparent that laminar/turbulent transition could be delayed up to a Reynolds number well over 5,000

by the proper combination of Stokes number and oscillatory amplitude because transition occurs much later than indicated by the stability criterion. In the present experimental program, runs 8, 9, and 12 with Reynolds numbers of 10, 826, 9445, and 10,135 show excellent agreement between experimental flow and calculated flow and prove that the present viscous theory is certainly applicable from the operational engineering approach to an effective Reynolds number of 10,000 and a Stokes number of 1,000.

CONCLUSIONS

The correspondence of measured and calculated flow rate provided verification of Womersley's method for the computation of instantaneous flow in an incompressible fluid. The limits of applicability remain undefined beyond the test range. Highly fluctuating experimental pressure gradient data have had little effect on calculated flow under the conditions of this experimentation. The analytical method is considered to be limited to cases where mean flow rate is a known quantity for practical reasons since the mean pressure gradient in most cases will not be distinguishable because of instrumentation limitations. A digital computer is deemed almost essential to flow computations by the method of Womersley. The complete Fortran computer program as used herein is given in the appendix.

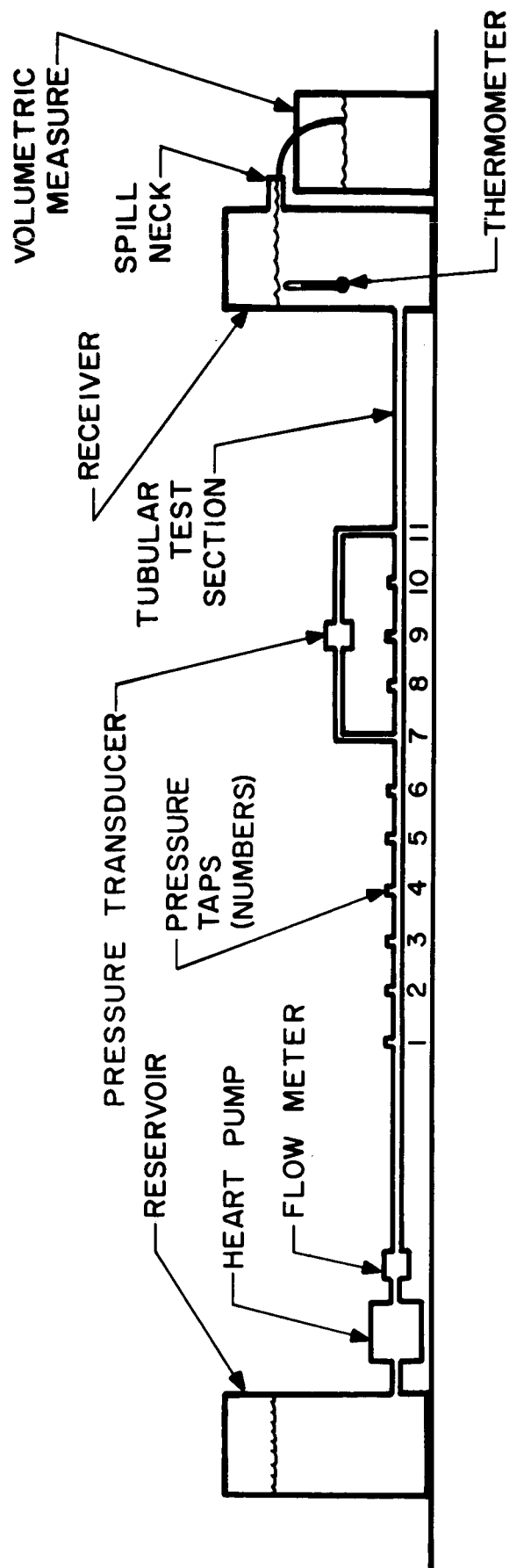


FIGURE 1. SCHEMATIC OF APPARATUS

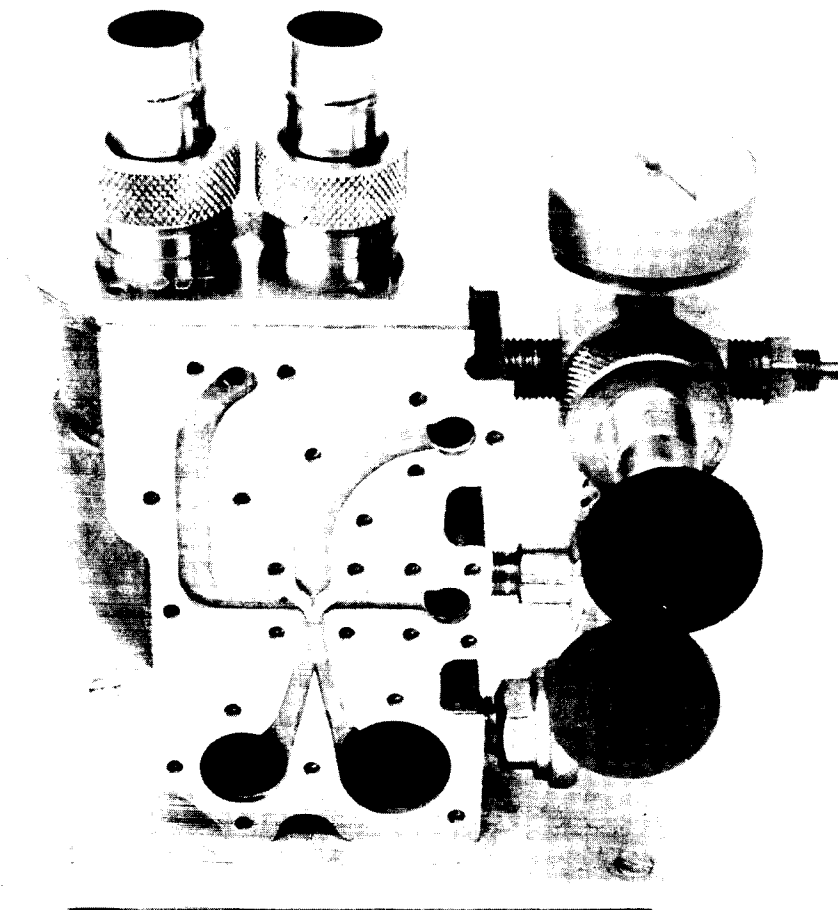


FIGURE 2. FLUIDIC HEART PUMP WITH COVER REMOVED



FIGURE 3. PERISTALTIC HEART PUMP

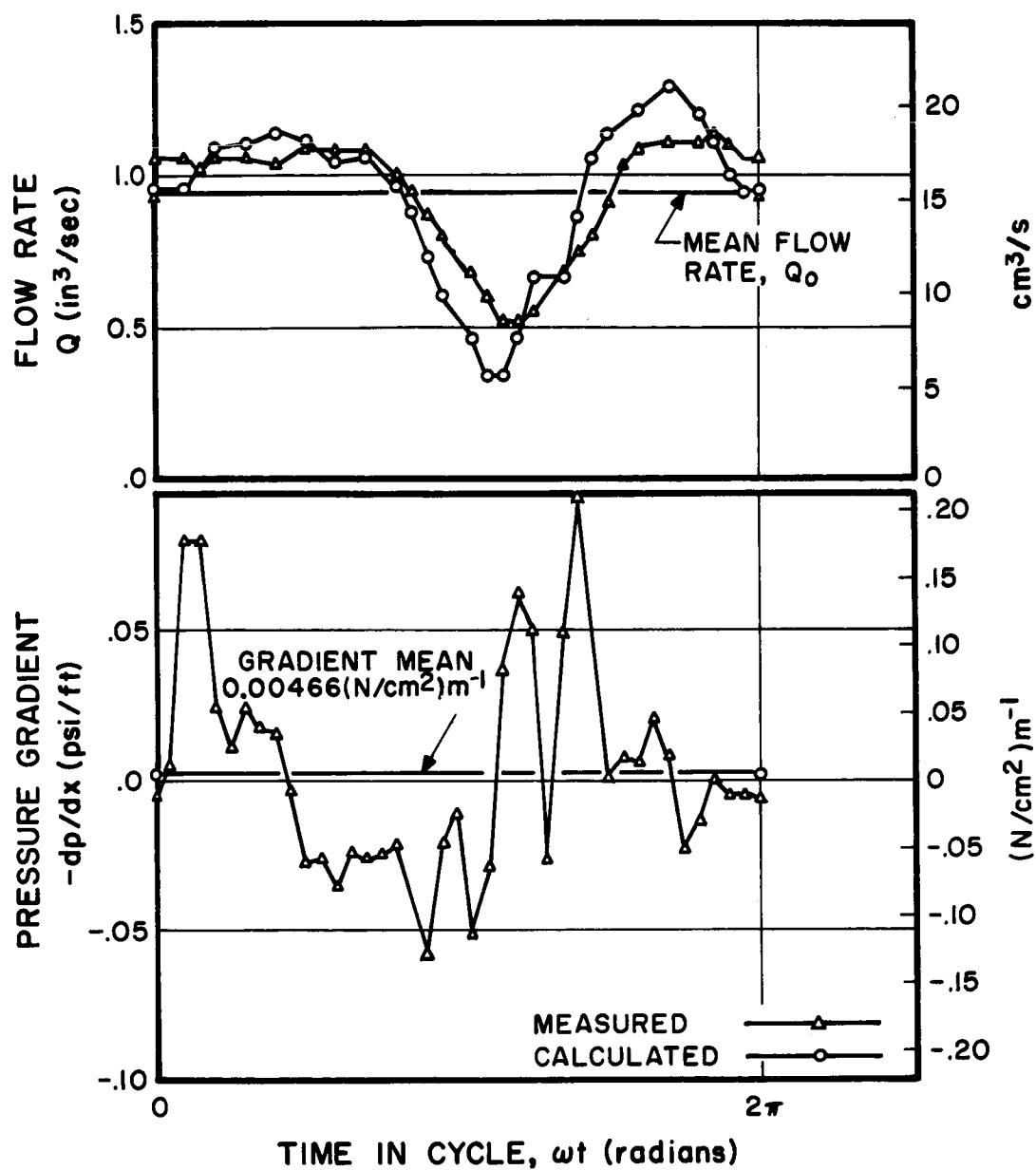


FIGURE 4. RUN 1. MEASURED PRESSURE GRADIENT, MEASURED FLOW RATE, AND COMPUTED FLOW RATE USING PERISTALTIC HEART PUMP. STOKES NUMBER 870; EFFECTIVE REYNOLDS NUMBER 1566; PULSE FREQUENCY 1.27 Hz

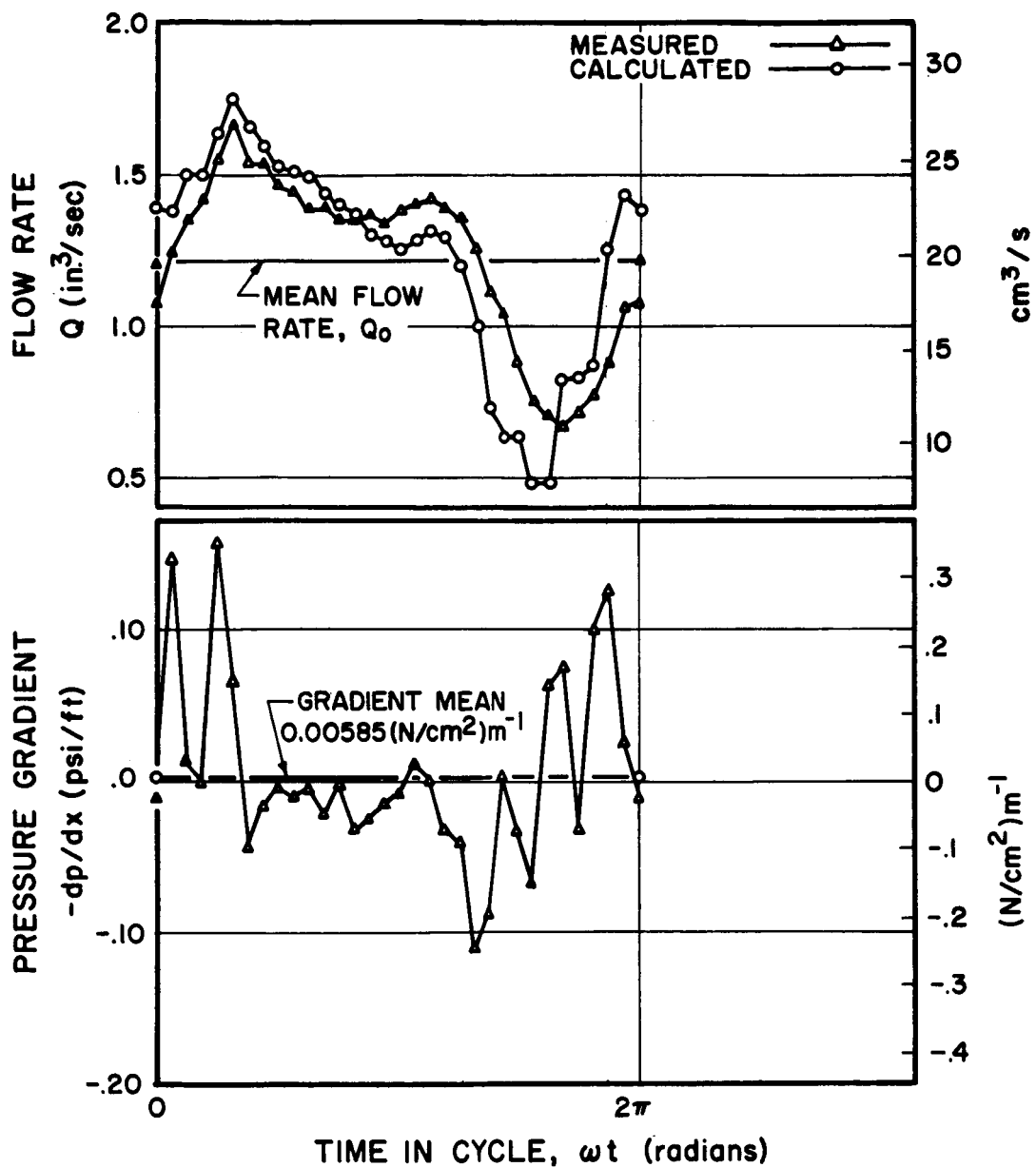


FIGURE 5. RUN 2. MEASURED PRESSURE GRADIENT, MEASURED FLOW RATE, AND COMPUTED FLOW RATE USING PERISTALTIC HEART PUMP. STOKES NUMBER 1089; EFFECTIVE REYNOLDS NUMBER 2033; PULSE FREQUENCY 1.59 Hz

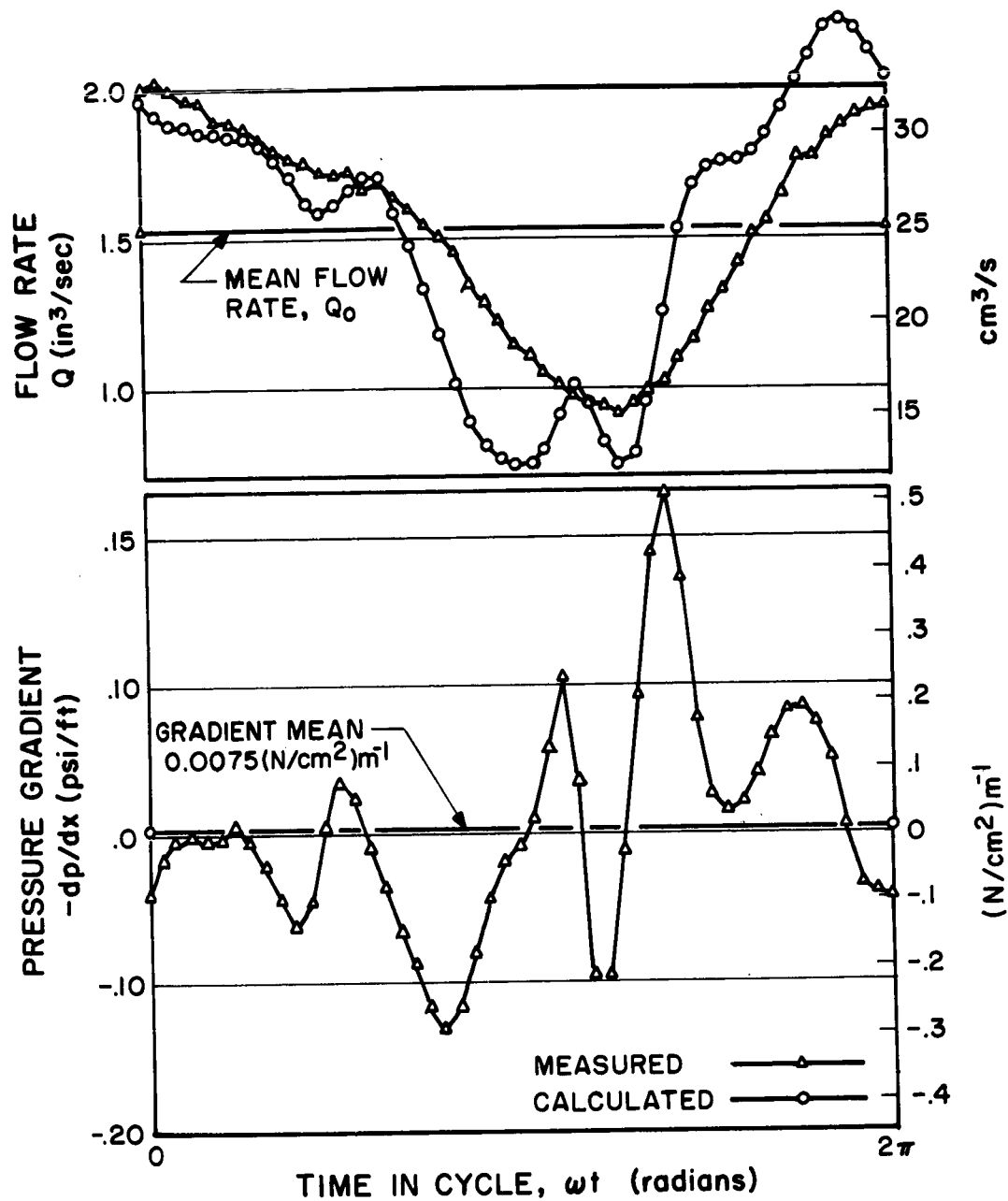


FIGURE 6. RUN 3. MEASURED PRESSURE GRADIENT, MEASURED FLOW RATE, AND COMPUTED FLOW RATE USING PERISTALTIC HEART PUMP. STOKES NUMBER 1347; EFFECTIVE REYNOLDS NUMBER 2538; PULSE FREQUENCY 1.96 Hz

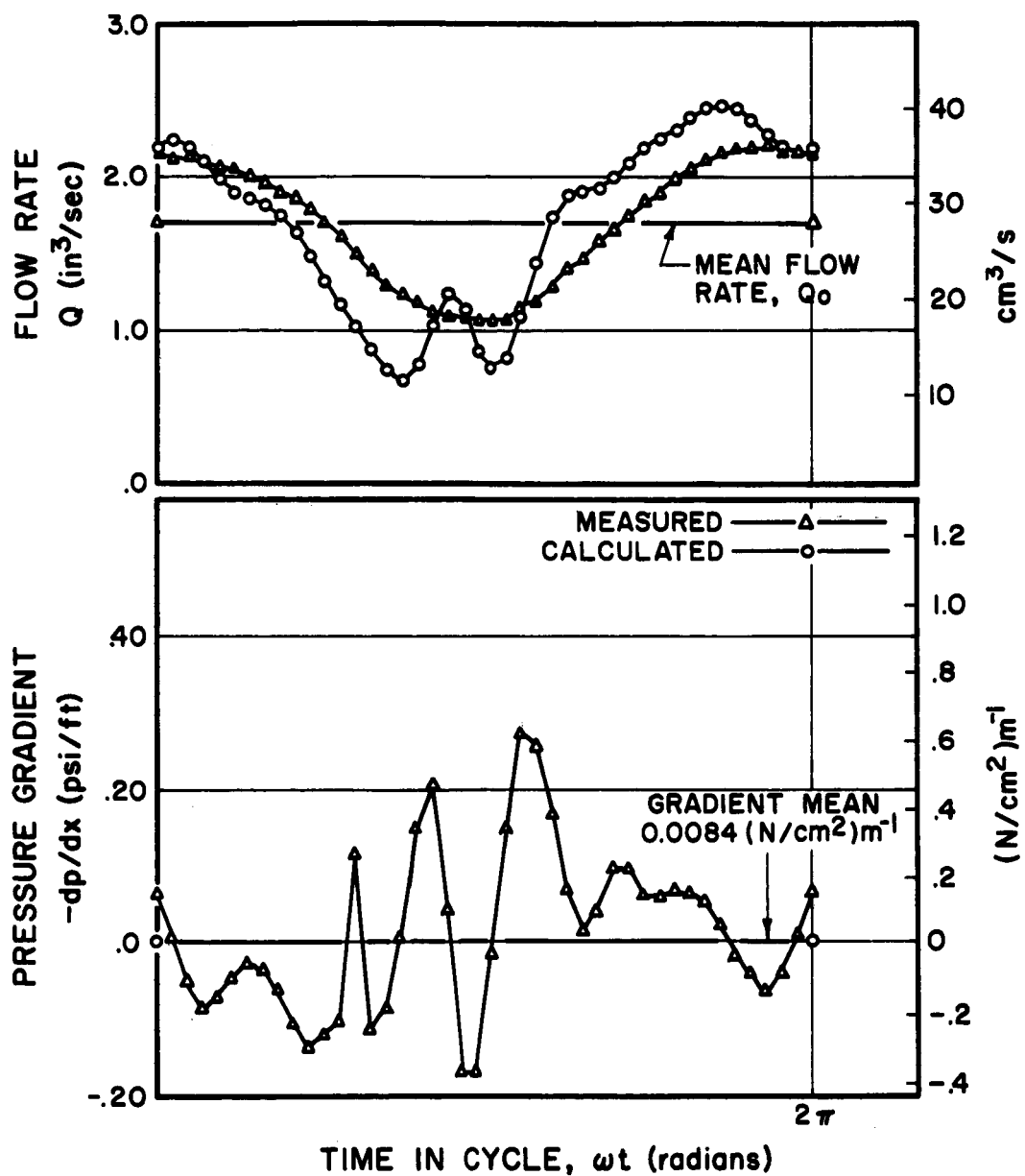


FIGURE 7. RUN 4. MEASURED PRESSURE GRADIENT, MEASURED FLOW RATE, AND COMPUTED FLOW RATE USING PERISTALTIC HEART PUMP. STOKES NUMBER 1597; EFFECTIVE REYNOLDS NUMBER 2819; PULSE FREQUENCY 2.33 Hz

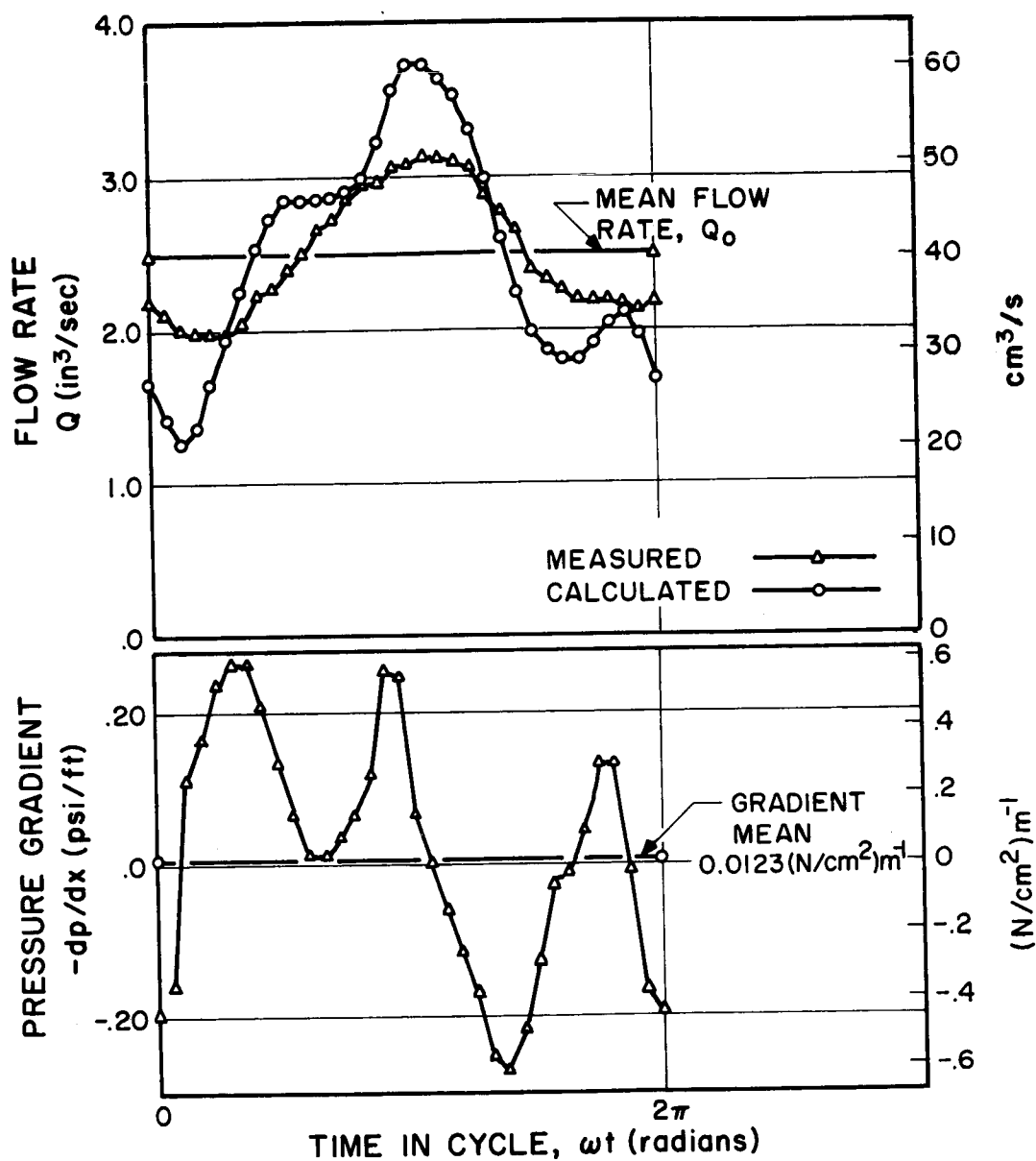


FIGURE 8. RUN 5. MEASURED PRESSURE GRADIENT, MEASURED FLOW RATE, AND COMPUTED FLOW RATE USING PERISTALTIC HEART PUMP. STOKES NUMBER 2078; EFFECTIVE REYNOLDS NUMBER 4143; PULSE FREQUENCY 3.03 Hz

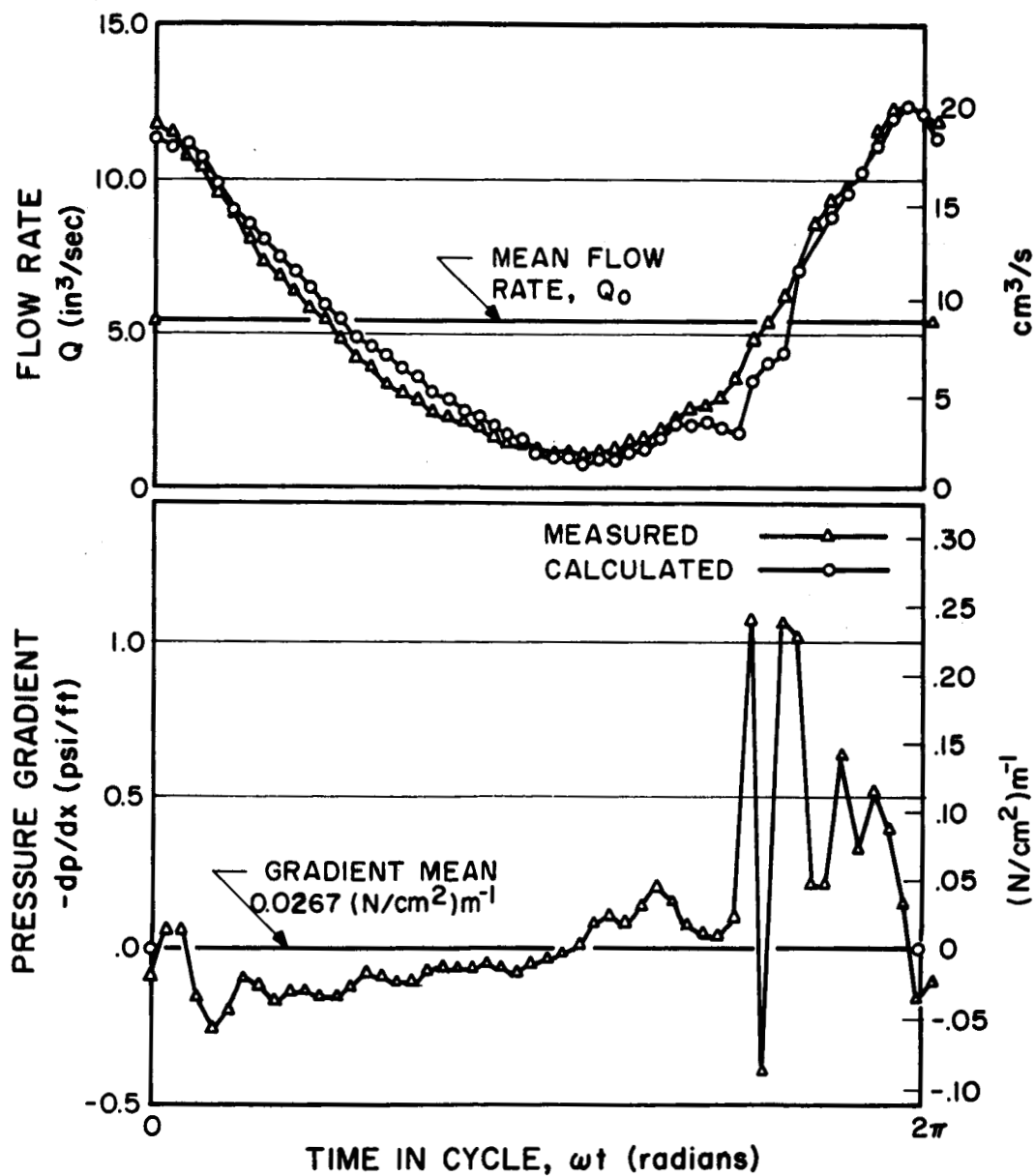


FIGURE 9. RUN 6. MEASURED PRESSURE GRADIENT, MEASURED FLOW RATE, AND COMPUTED FLOW RATE USING FLUIDIC HEART PUMP. STOKES NUMBER 687; EFFECTIVE REYNOLDS NUMBER 8939; PULSE FREQUENCY 1.00 Hz

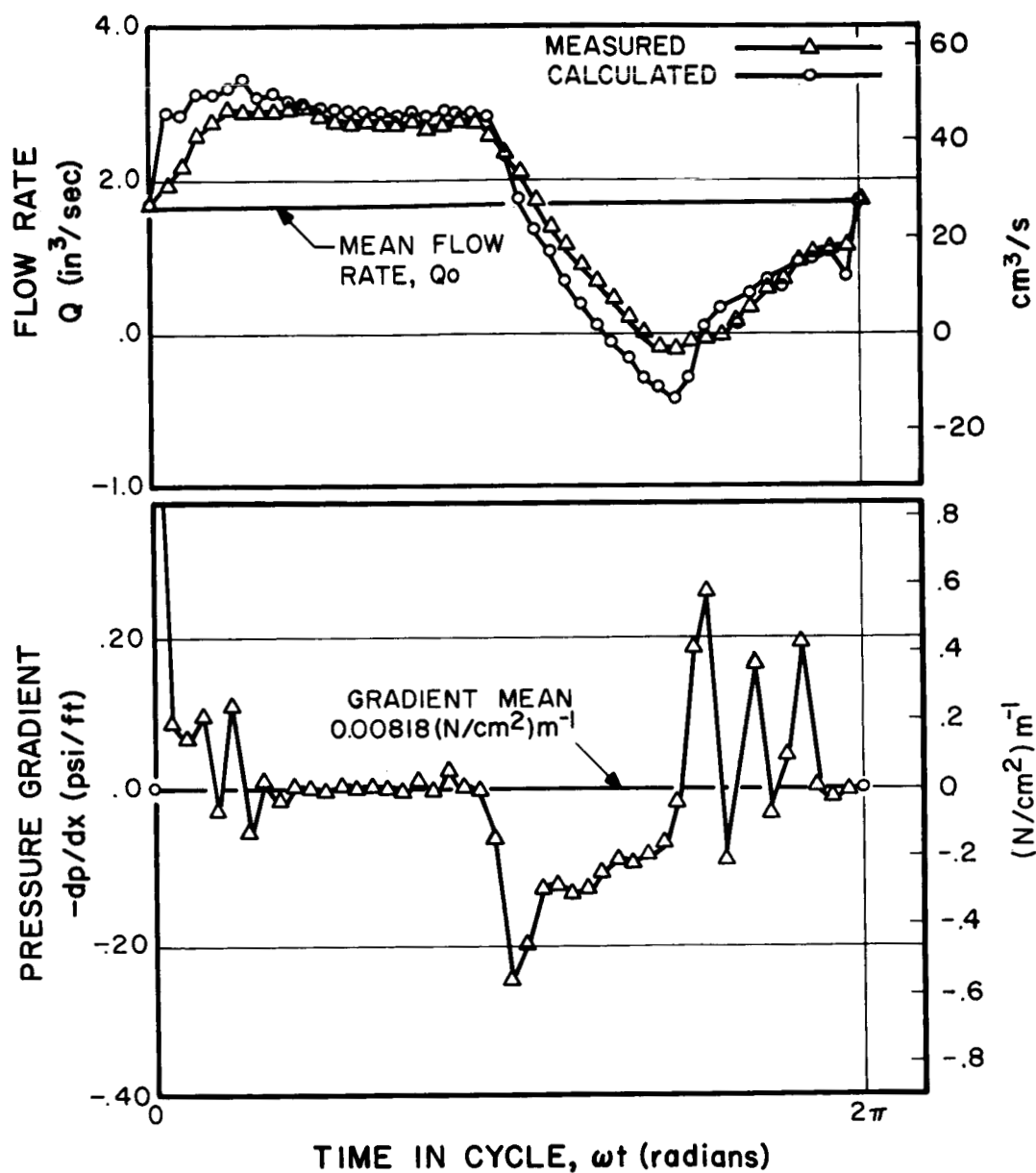


FIGURE 10. RUN 7. MEASURED PRESSURE GRADIENT, MEASURED FLOW RATE, AND COMPUTED FLOW RATE USING FLUIDIC HEART PUMP. STOKES NUMBER 758; EFFECTIVE REYNOLDS NUMBER 2787; PULSE FREQUENCY 1.09 Hz

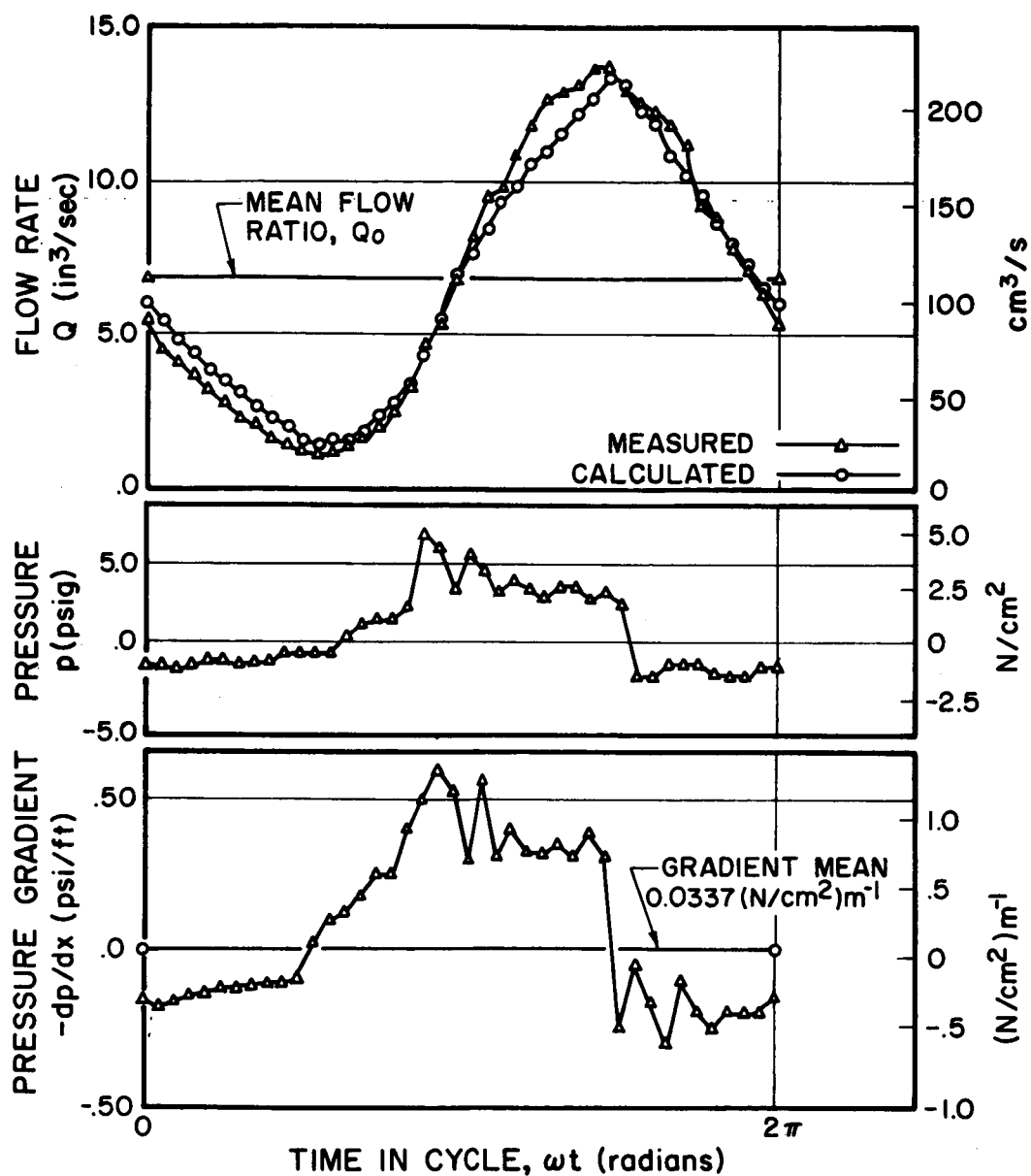


FIGURE 11. RUN 8. MEASURED PRESSURE GRADIENT, MEASURED PRESSURE, MEASURED FLOW RATE, AND COMPUTED FLOW RATE USING FLUIDIC HEART PUMP. STOKES NUMBER 803; EFFECTIVE REYNOLDS NUMBER 10 826; PULSE FREQUENCY 1.22 Hz

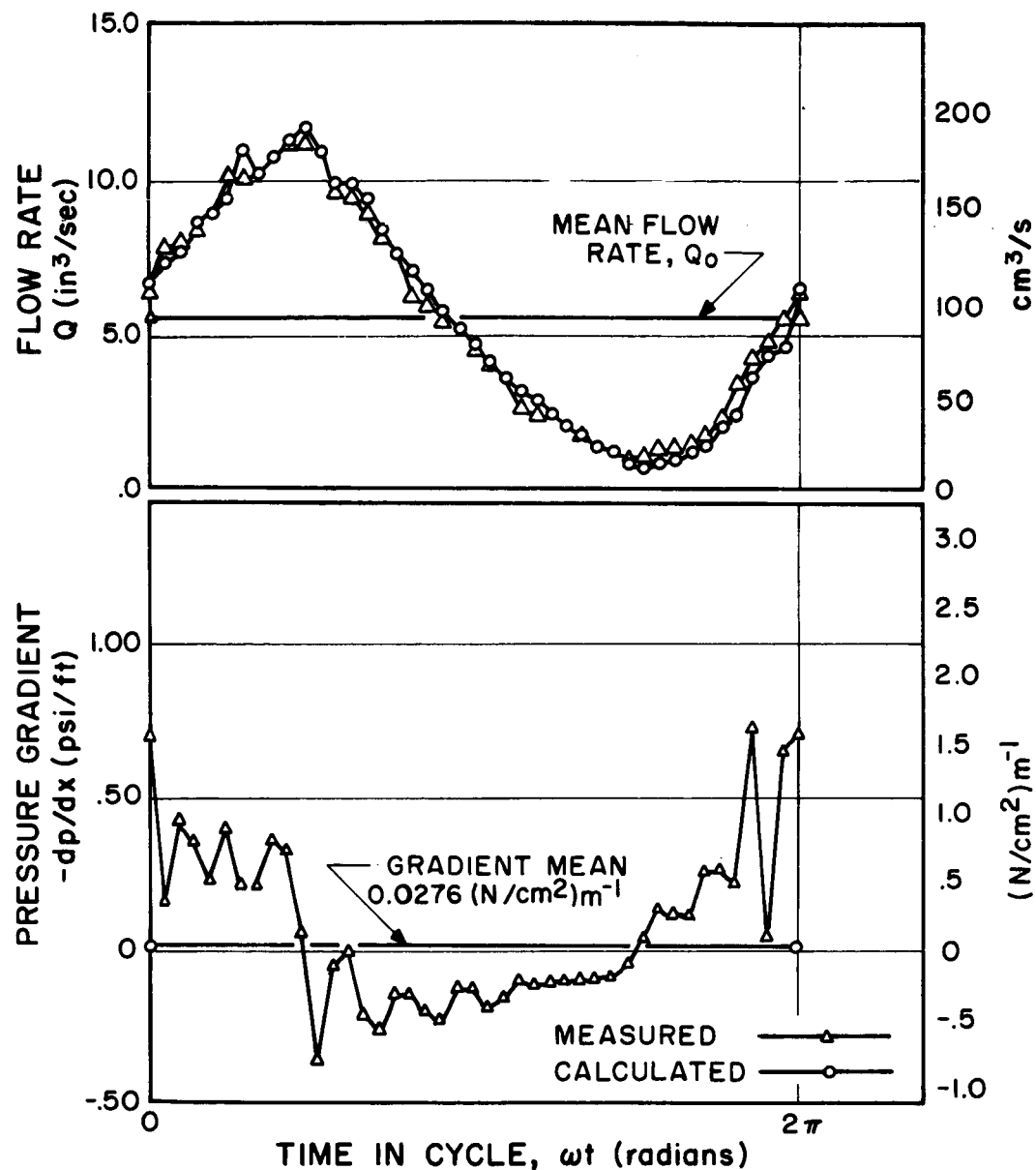


FIGURE 12. RUN 9. MEASURED PRESSURE GRADIENT, MEASURED FLOW RATE, AND COMPUTED FLOW RATE USING FLUIDIC HEART PUMP. STOKES NUMBER 837; EFFECTIVE REYNOLDS NUMBER 9445; PULSE FREQUENCY 1.19 Hz

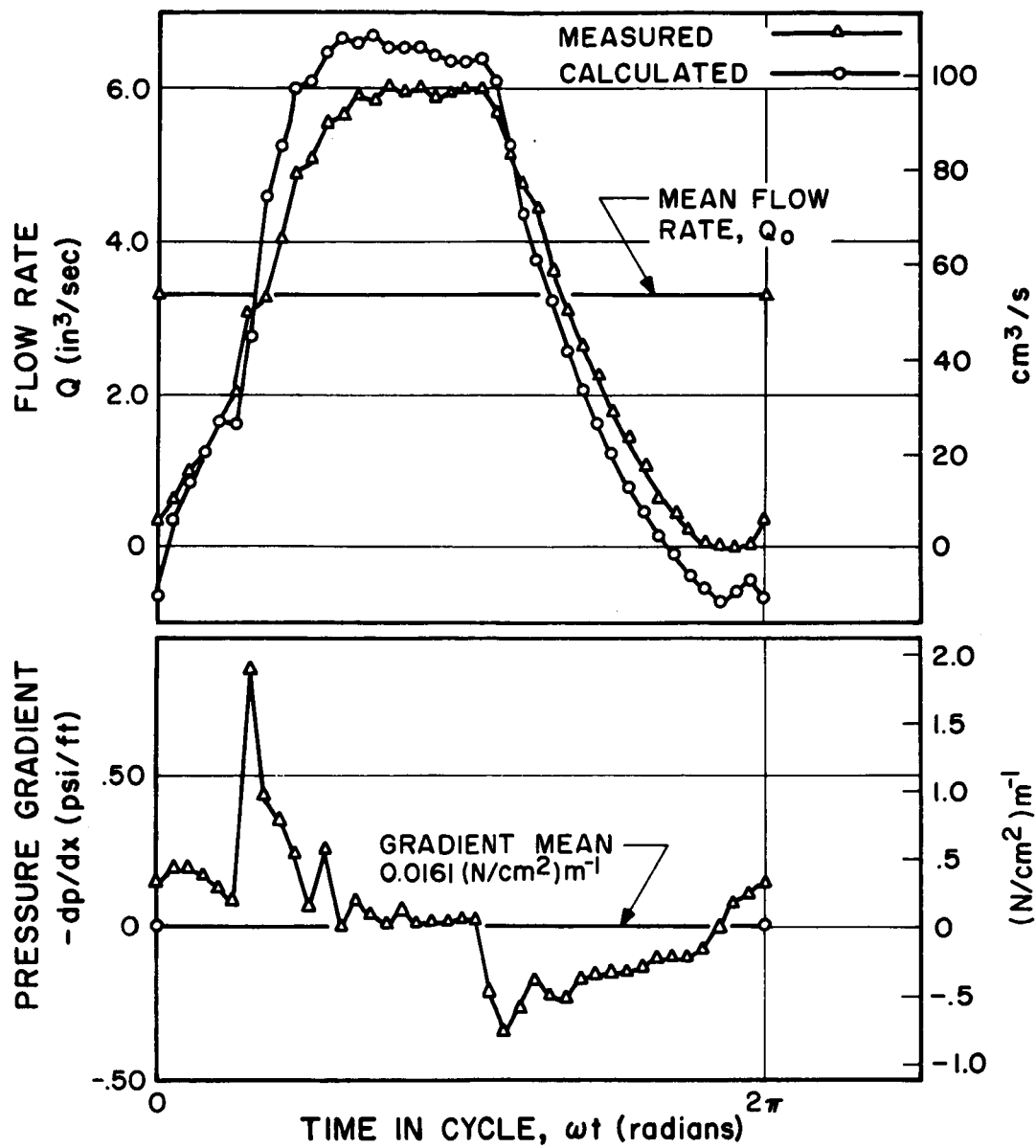


FIGURE 13. RUN 10. MEASURED PRESSURE GRADIENT, MEASURED FLOW RATE, AND COMPUTED FLOW RATE USING FLUIDIC HEART PUMP. STOKES NUMBER 872; EFFECTIVE REYNOLDS NUMBER 5535; PULSE FREQUENCY 1.25 Hz

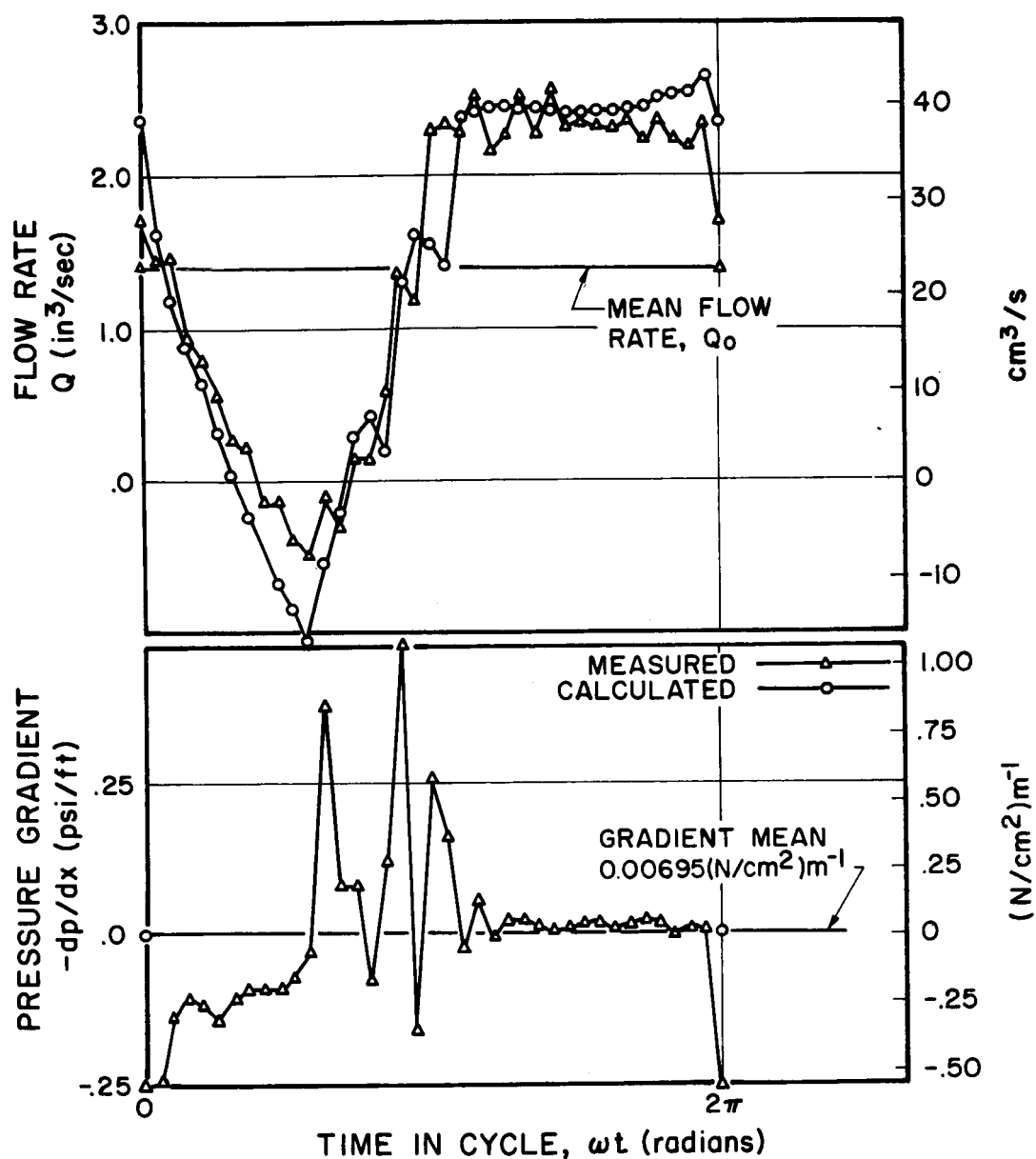


FIGURE 14. RUN 11. MEASURED PRESSURE GRADIENT, MEASURED FLOW RATE, AND COMPUTED FLOW RATE USING FLUIDIC HEART PUMP. STOKES NUMBER 902; EFFECTIVE REYNOLDS NUMBER 2324; PULSE FREQUENCY 1.32 Hz

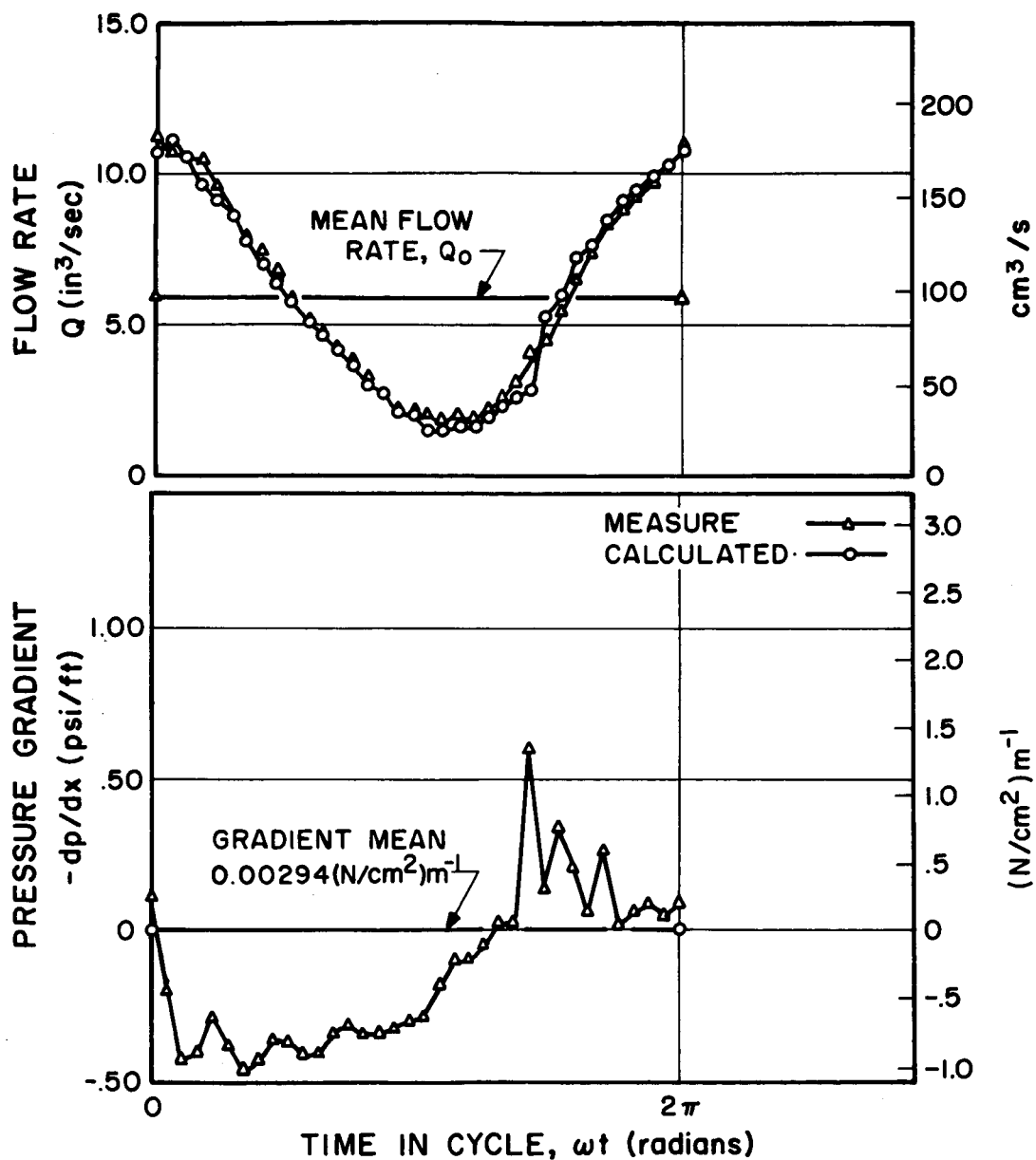


FIGURE 15. RUN 12. MEASURED PRESSURE GRADIENT, MEASURED FLOW RATE, AND COMPUTED FLOW RATE USING FLUIDIC HEART PUMP. STOKES NUMBER 1009; EFFECTIVE REYNOLDS NUMBER 10 135; PULSE FREQUENCY 1.43 Hz

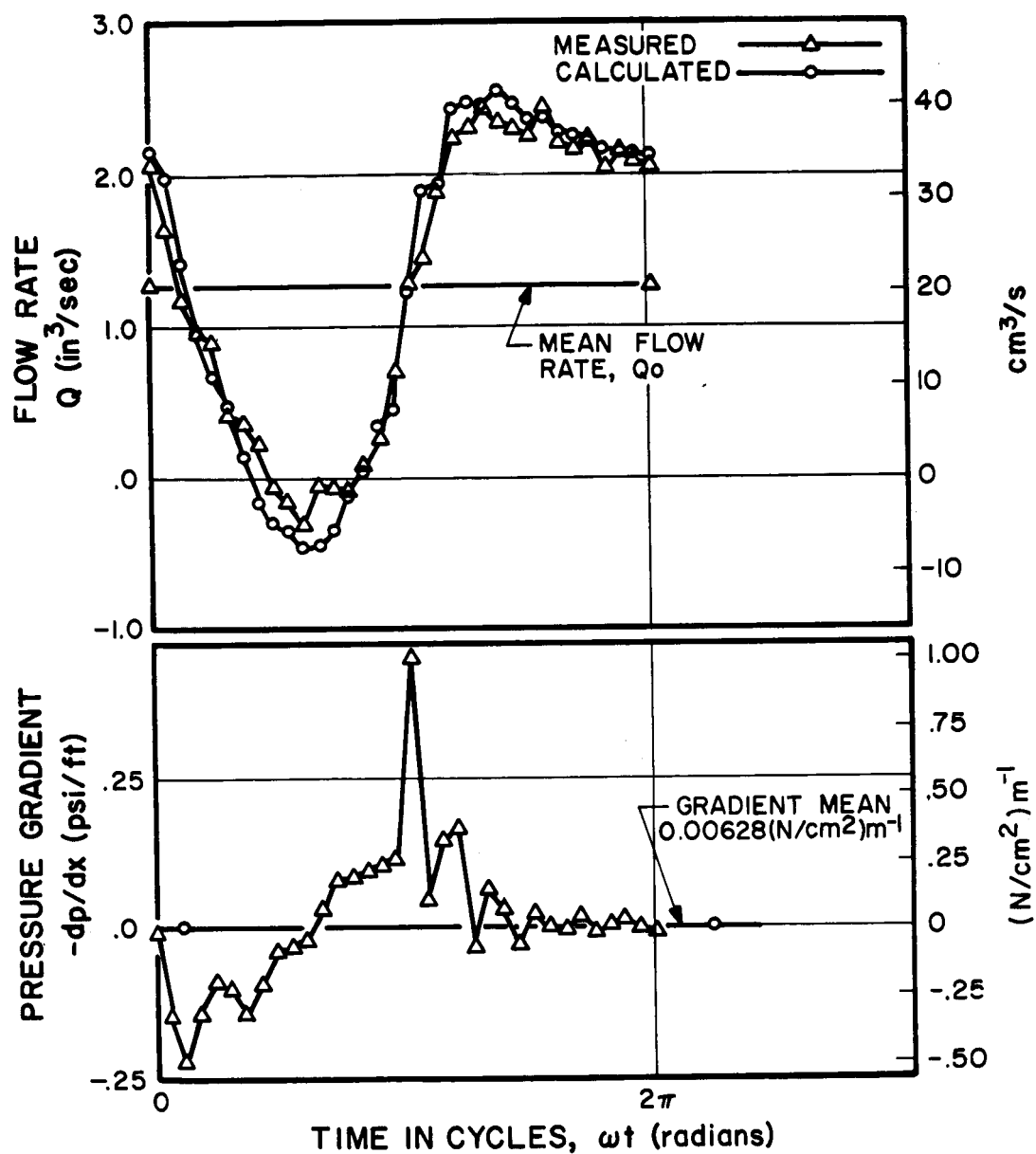


FIGURE 16. RUN 13. MEASURED PRESSURE GRADIENT, MEASURED FLOW RATE, AND COMPUTED FLOW RATE USING FLUIDIC HEART PUMP. STOKES NUMBER 1039; EFFECTIVE REYNOLDS NUMBER 2107; PULSE FREQUENCY 1.52 Hz

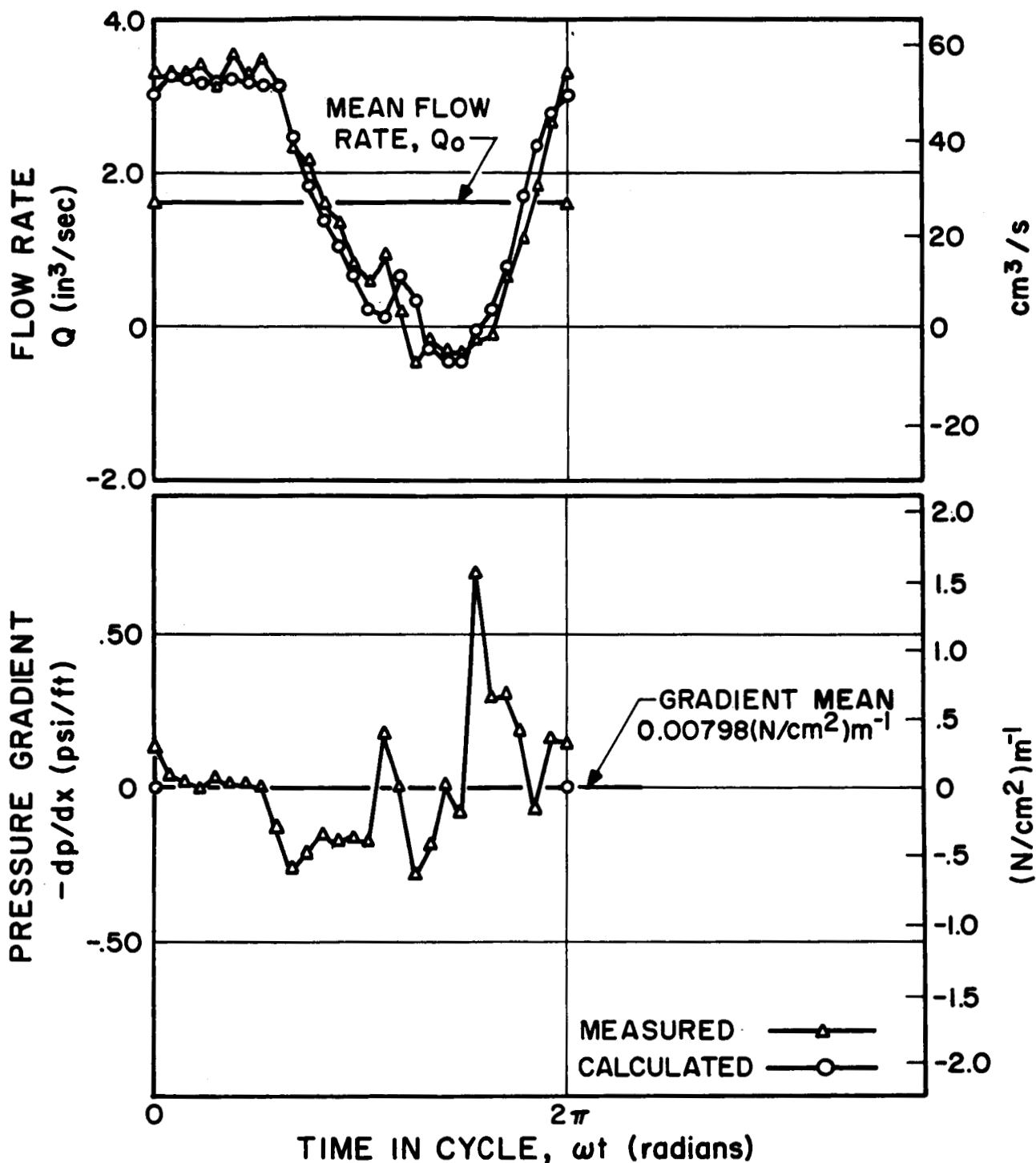


FIGURE 17. RUN 14. MEASURED PRESSURE GRADIENT, MEASURED FLOW RATE, AND COMPUTED FLOW RATE USING FLUIDIC HEART PUMP. STOKES NUMBER 1353; EFFECTIVE REYNOLDS NUMBER 2798; PULSE FREQUENCY 1.89 Hz

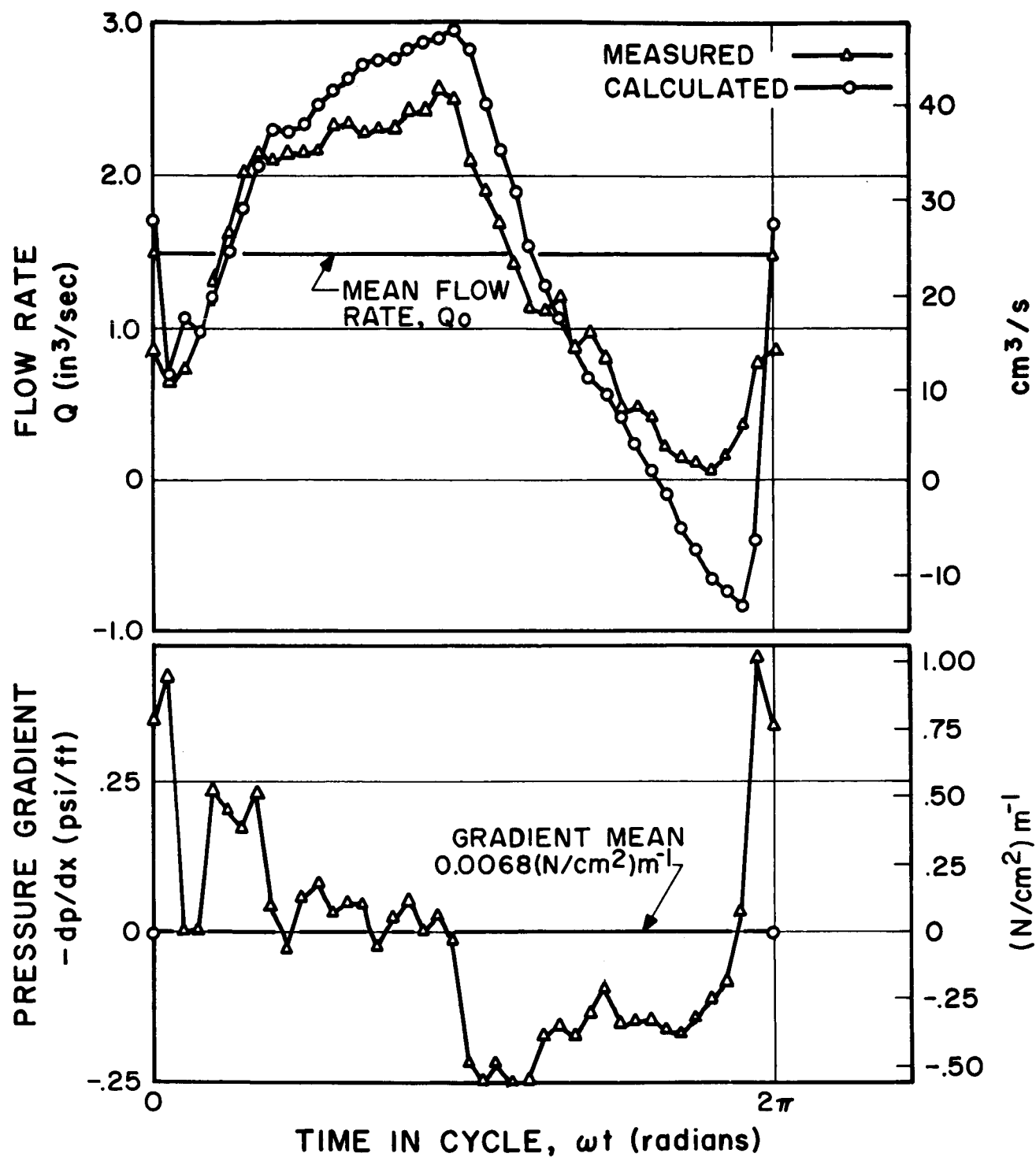


FIGURE 18. RUN 15. MEASURED PRESSURE GRADIENT, MEASURED FLOW RATE, AND COMPUTED FLOW RATE USING FLUIDIC HEART PUMP. STOKES NUMBER 1648; EFFECTIVE REYNOLDS NUMBER 2051; PULSE FREQUENCY 2.44 Hz

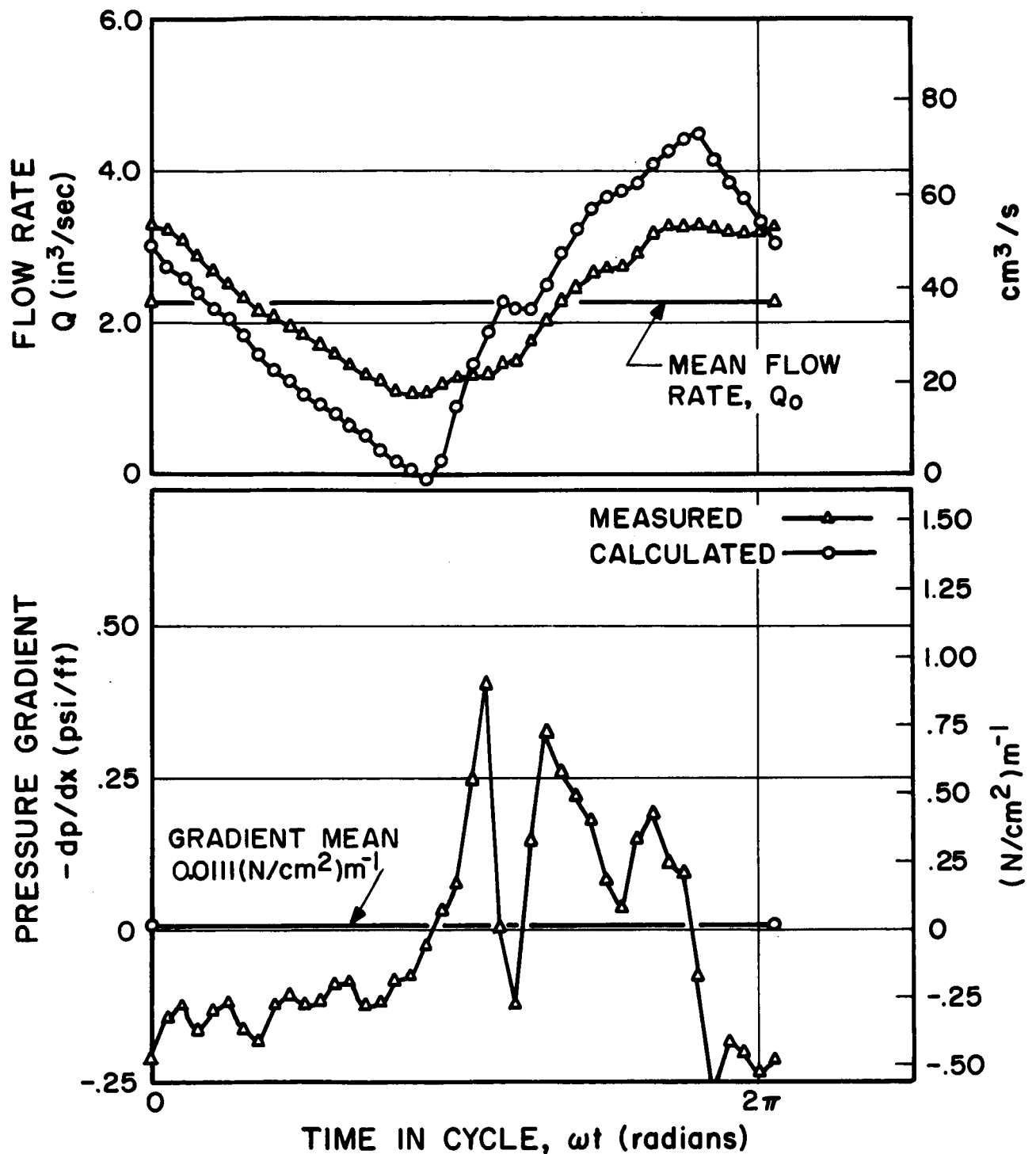


FIGURE 19. RUN 16. MEASURED PRESSURE GRADIENT, MEASURED FLOW RATE, AND COMPUTED FLOW RATE USING FLUIDIC HEART PUMP. STOKES NUMBER 1724; EFFECTIVE REYNOLDS NUMBER 3842; PULSE FREQUENCY 2.44 Hz

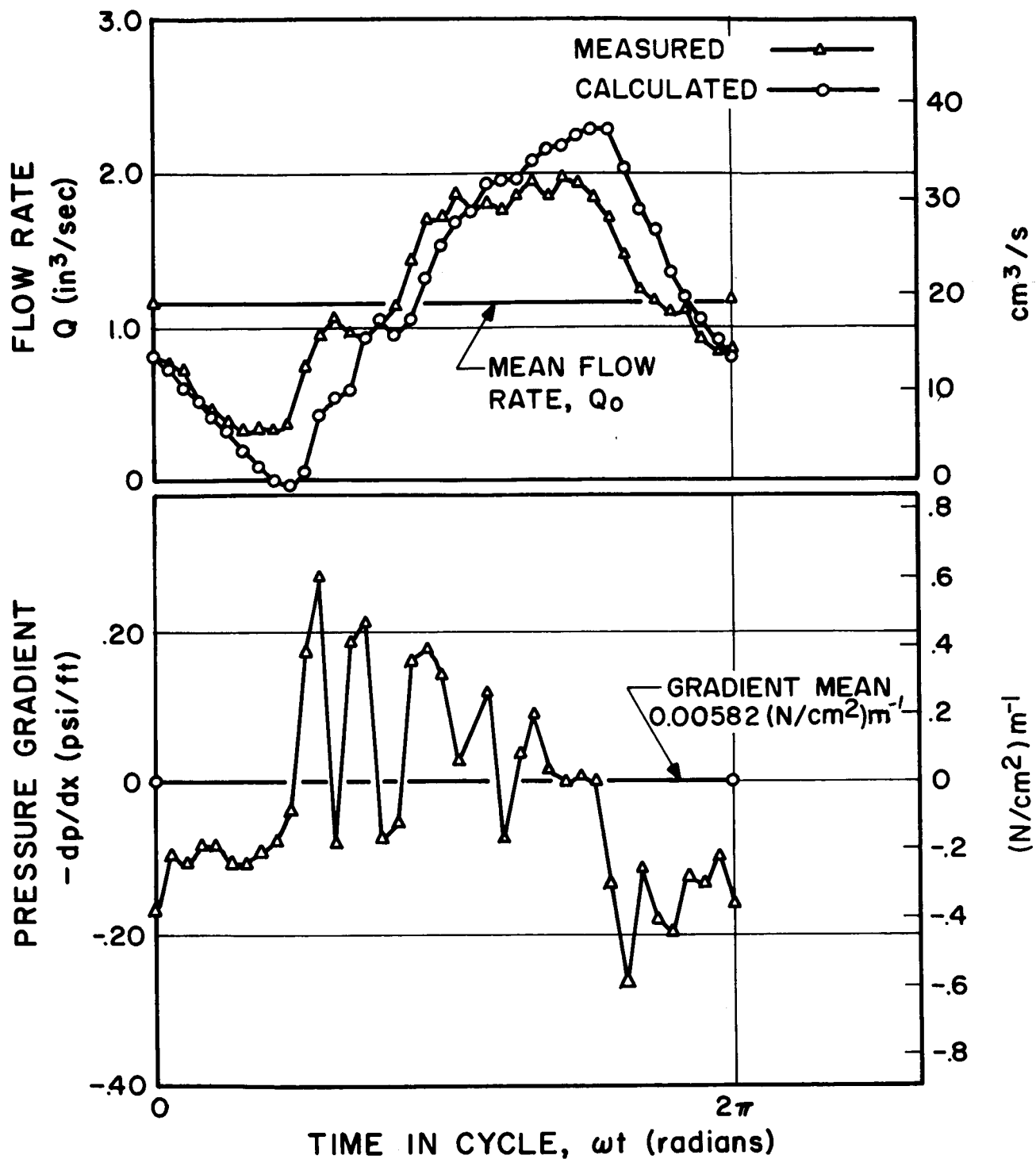


FIGURE 20. RUN 17. MEASURED PRESSURE GRADIENT, MEASURED FLOW RATE, AND COMPUTED FLOW RATE USING FLUIDIC HEART PUMP. STOKES NUMBER 1782; EFFECTIVE REYNOLDS NUMBER 1923; PULSE FREQUENCY 2.63 Hz

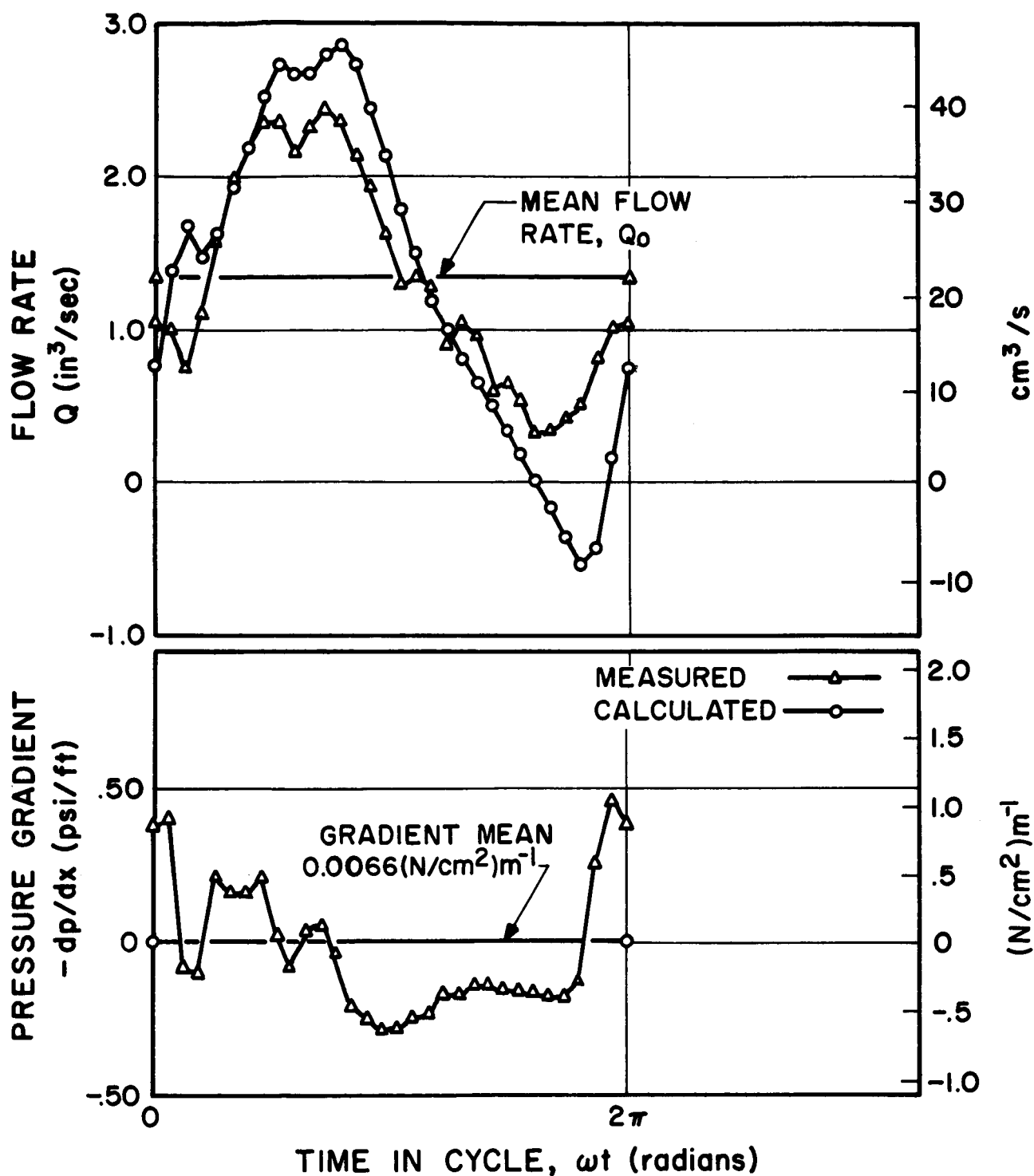


FIGURE 21. RUN 18. MEASURED PRESSURE GRADIENT, MEASURED FLOW RATE, AND COMPUTED FLOW RATE USING FLUIDIC HEART PUMP. STOKES NUMBER 2050; EFFECTIVE REYNOLDS NUMBER 2070; PULSE FREQUENCY 3.20 Hz

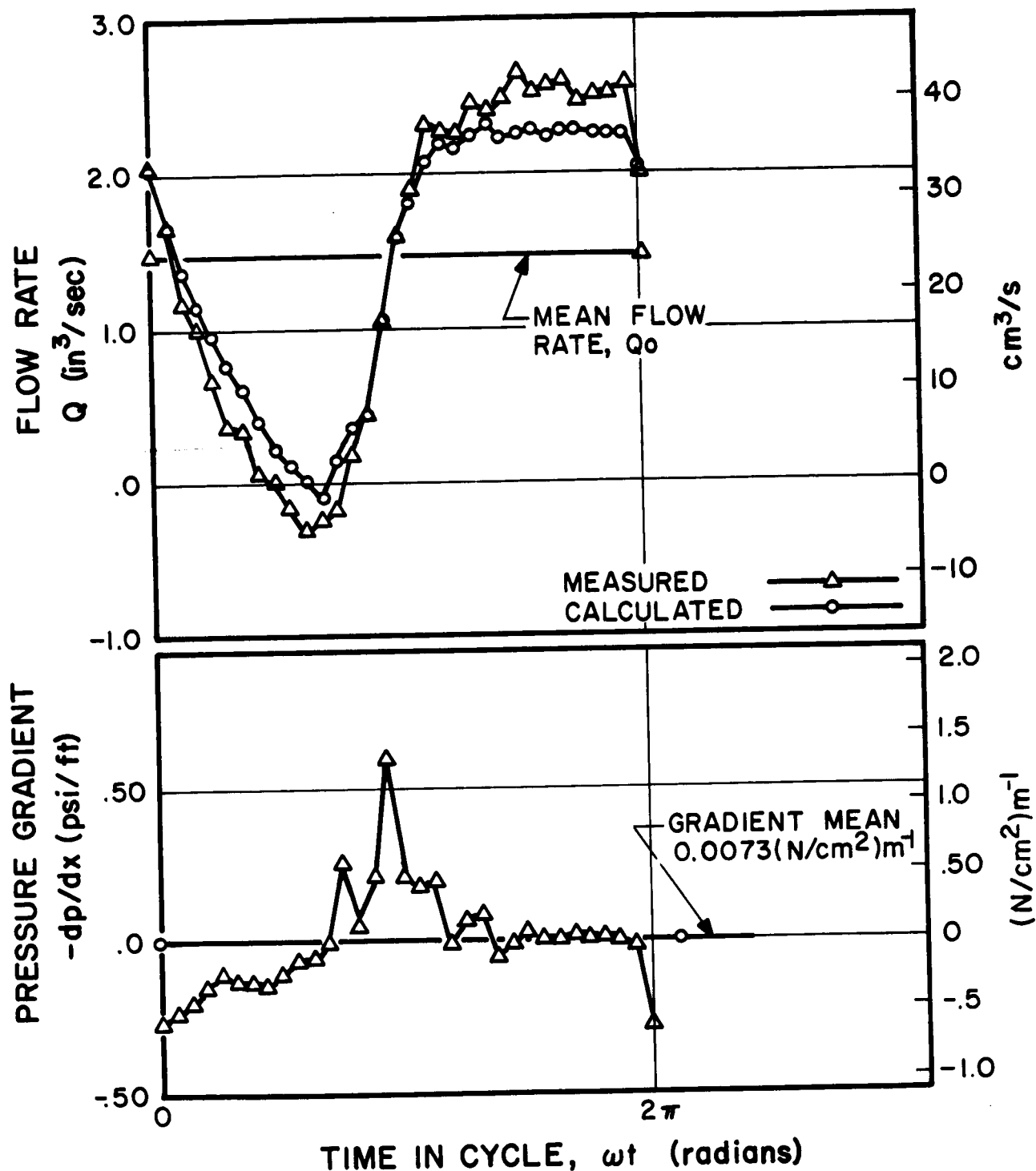


FIGURE 22. RUN 19. MEASURED PRESSURE GRADIENT, MEASURED FLOW RATE, AND COMPUTED FLOW RATE USING FLUIDIC HEART PUMP. STOKES NUMBER 2112; EFFECTIVE REYNOLDS NUMBER 2345; PULSE FREQUENCY 3.13 Hz

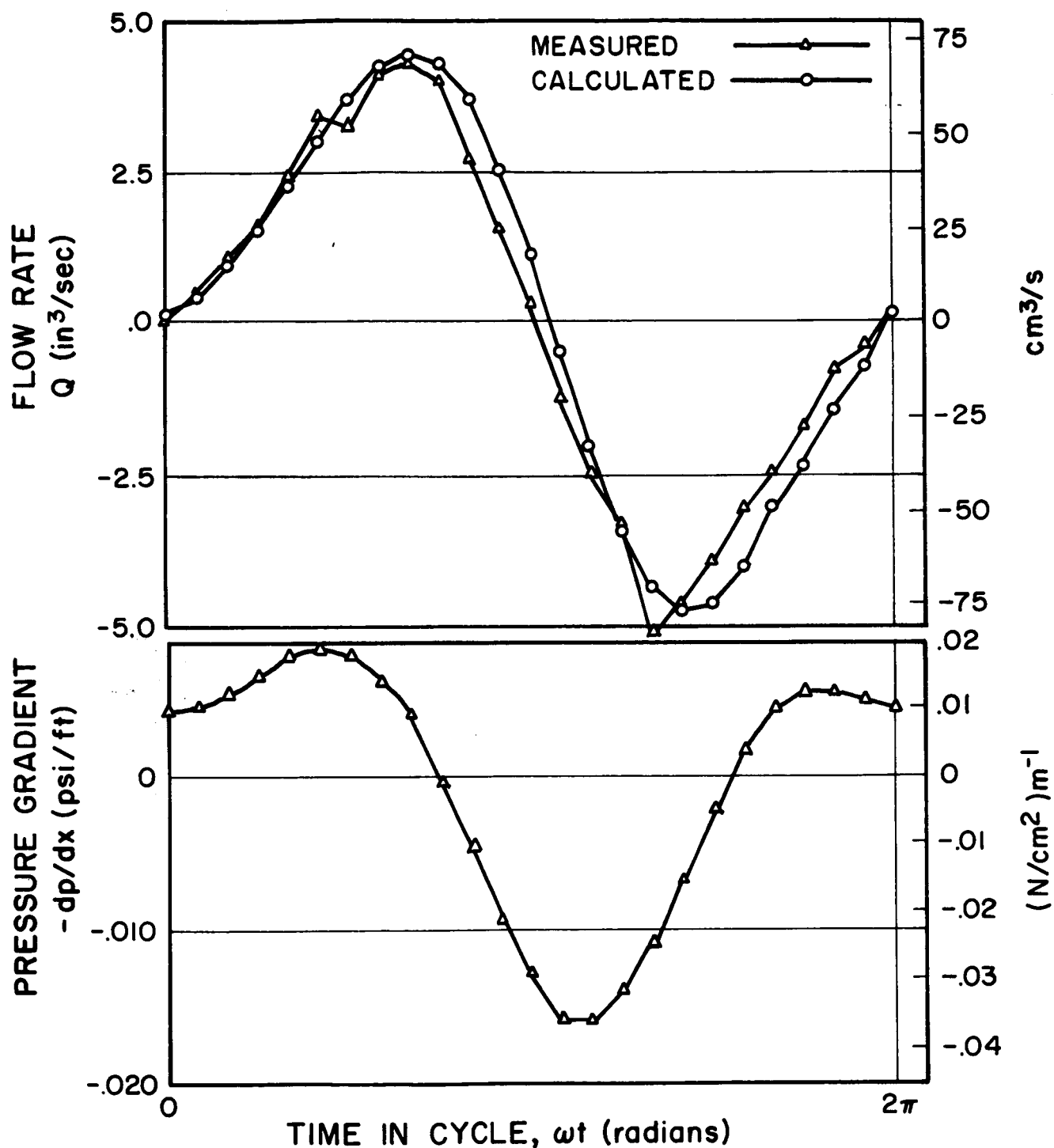


FIGURE 23. RUN 20. MEASURED PRESSURE GRADIENT,
MEASURED FLOW RATE, AND COMPUTED FLOW RATE USING
LINFORD EXPERIMENT DATA. STOKES NUMBER 77;
PULSE FREQUENCY 0.214 Hz

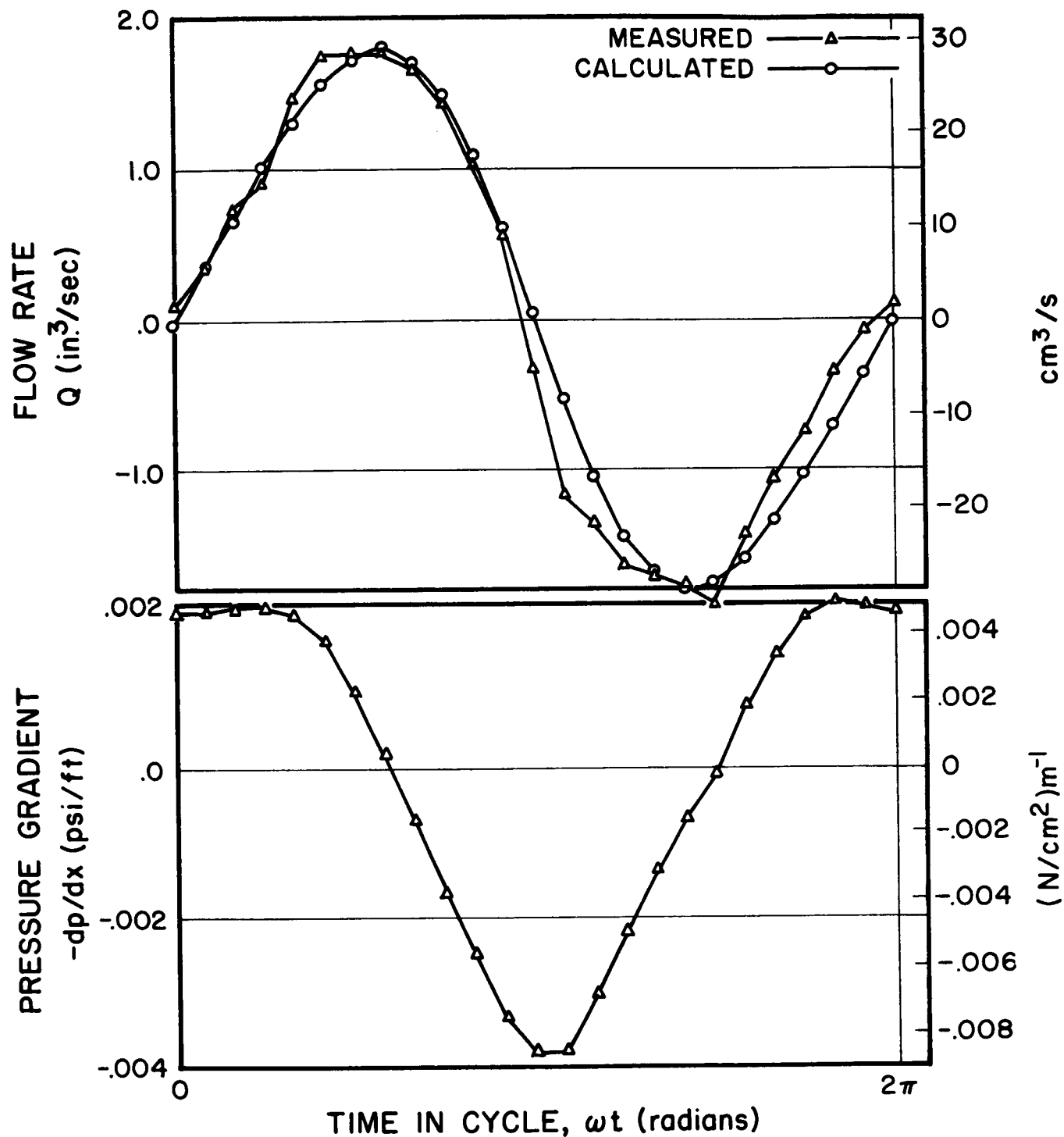


FIGURE 24. RUN 21. MEASURED PRESSURE GRADIENT, MEASURED FLOW RATE, AND COMPUTED FLOW RATE USING LINFORD EXPERIMENTAL DATA. STOKES NUMBER 778; EFFECTIVE REYNOLDS NUMBER 0; PULSE FREQUENCY 0.169 Hz

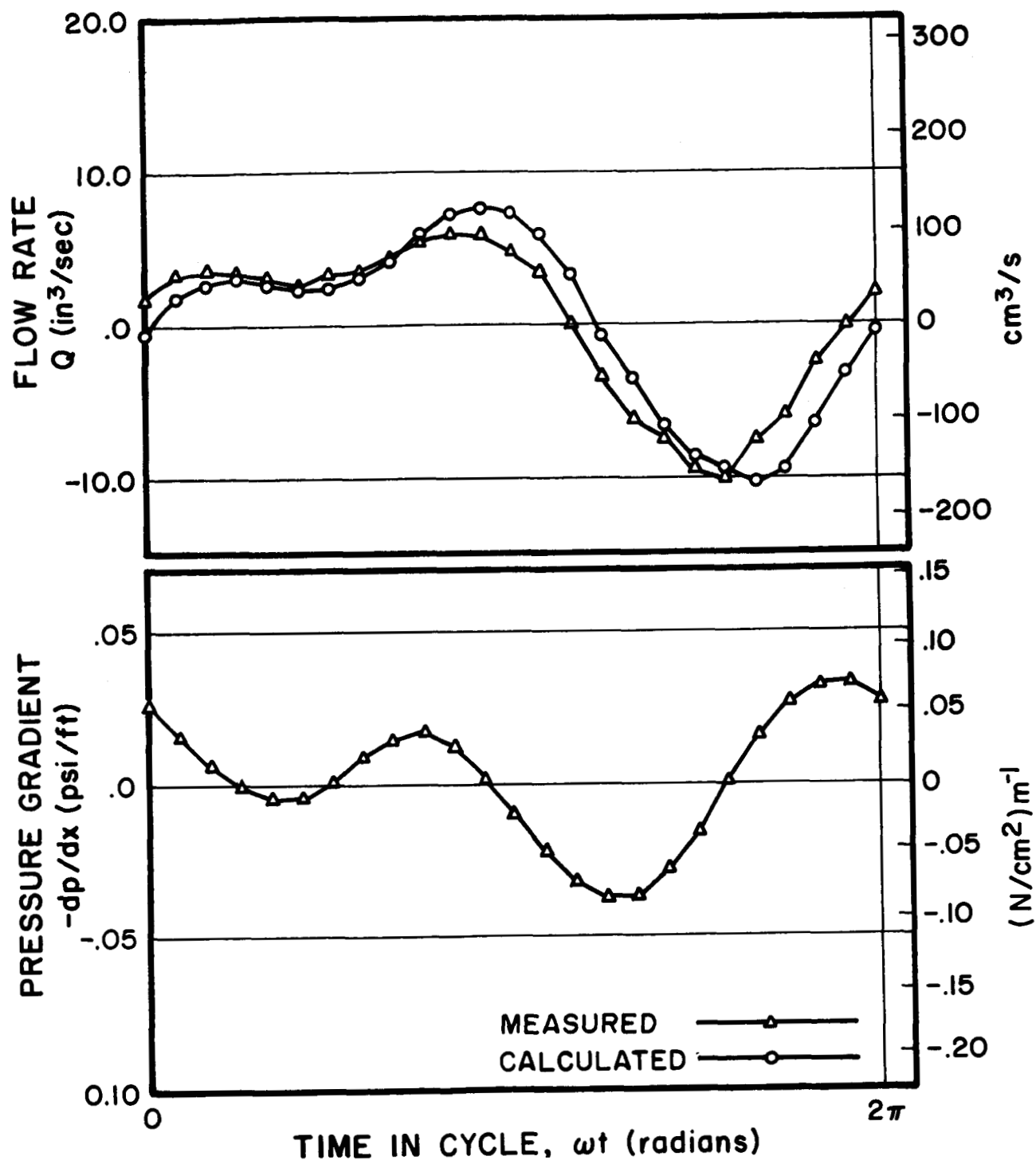


FIGURE 25. RUN 22. MEASURED PRESSURE GRADIENT, MEASURED FLOW RATE, AND COMPUTED FLOW RATE USING LINFORD EXPERIMENTAL DATA. STOKES NUMBER 1774; PULSE FREQUENCY 0.309 Hz

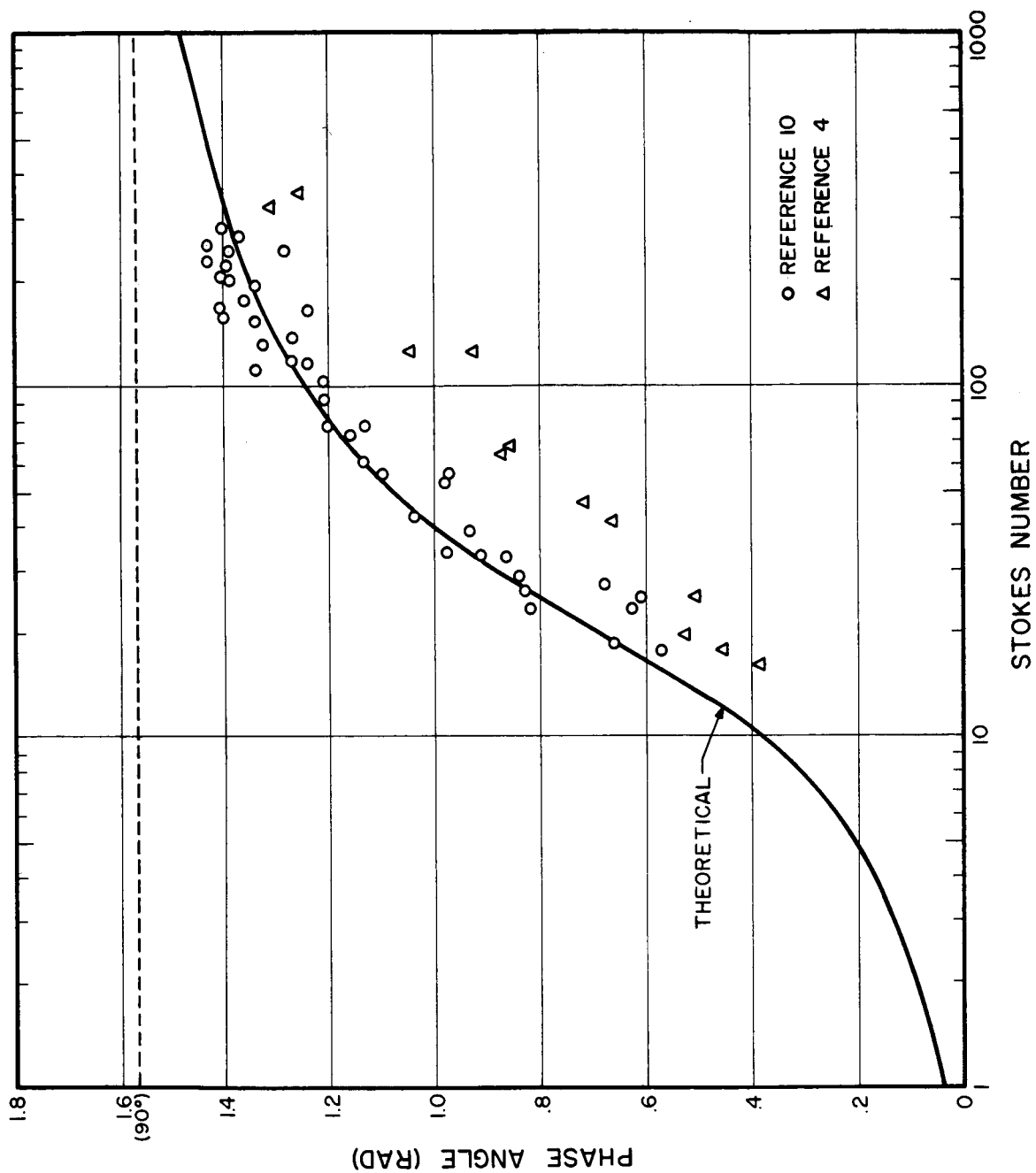


FIGURE 26. PHASE SHIFT ANGLE AGAINST STOKES NUMBER
FOR SINUSOIDAL OSCILLATORY PIPE FLOW

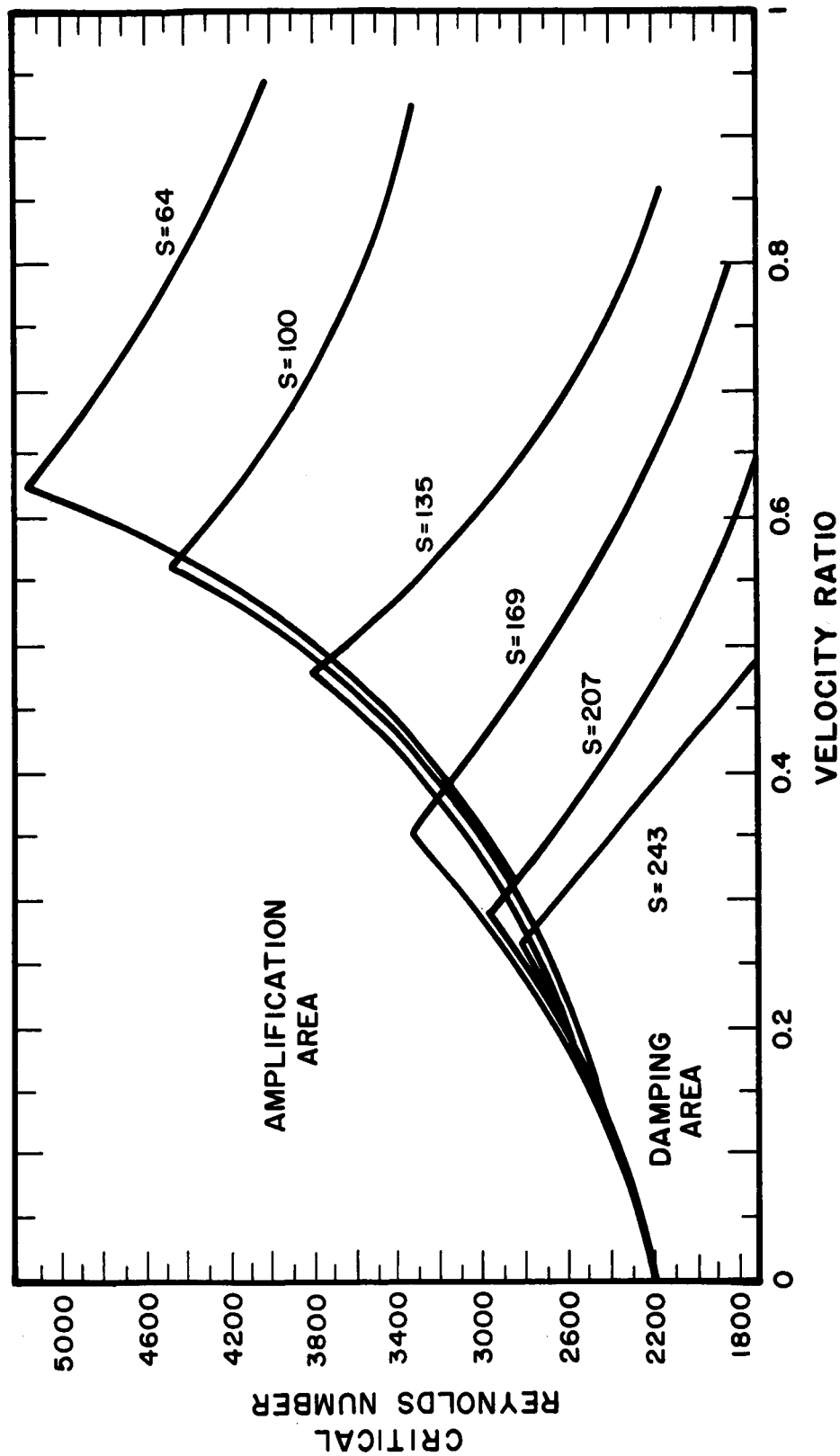


FIGURE 27. CRITICAL REYNOLDS NUMBER VERSUS VELOCITY RATIO FOR VARIOUS VALUES OF STOKES NUMBER

APPENDIX – FORTRAN COMPUTER PROGRAM

Macro Flow Chart of Digital Computer Program and Subroutines

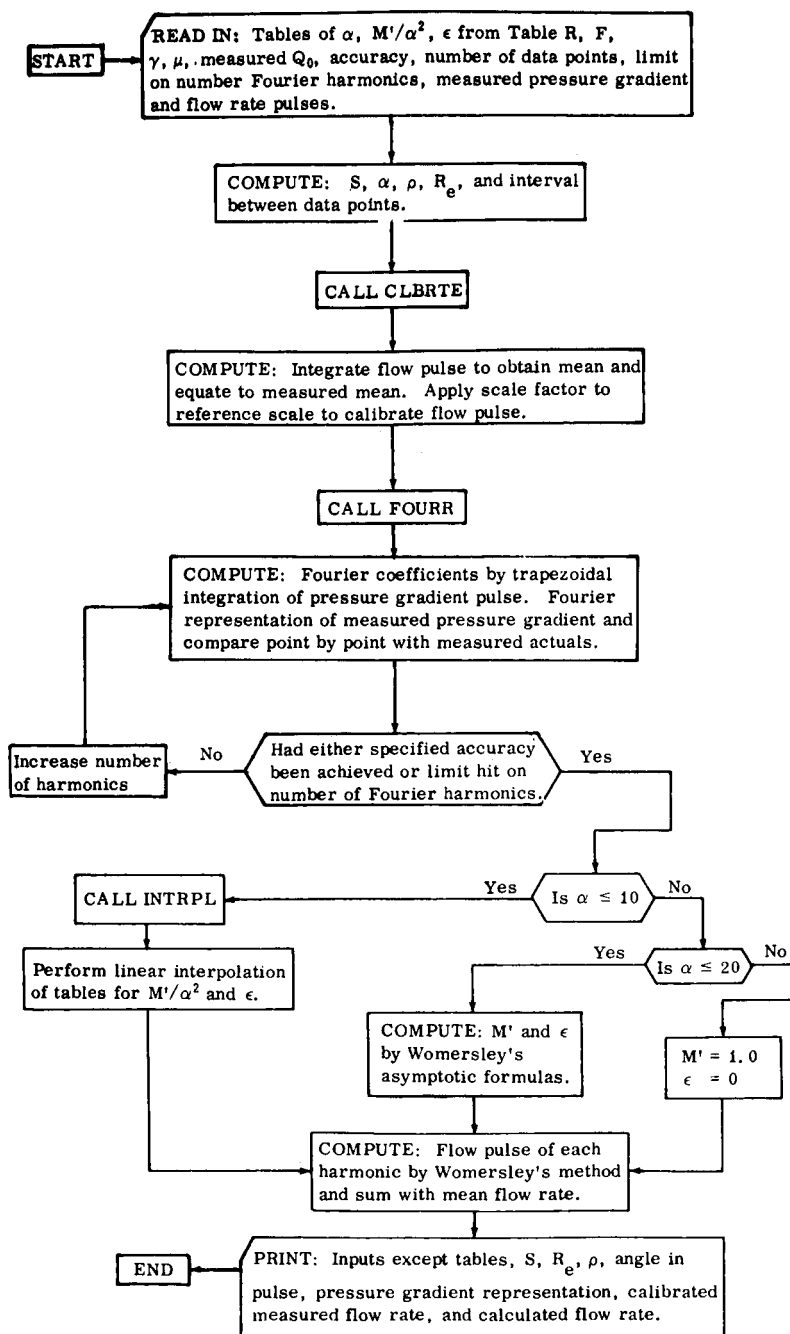


Table of Parameters

The following table gives amplitude parameters and phase angle complements for frequency parameters from zero to ten.

α	M'/α^2	ϵ	α	M'/α^2	ϵ	α	M'/α^2	ϵ	α	M'/α^2	ϵ
0.00	0.1250	90.00	2.50	0.0855	44.93	5.00	0.0302	18.65	7.50	0.0147	11.87
.05	.1250	89.98	2.55	.0837	43.98	5.05	.0297	18.43	7.55	.0146	11.78
.10	.1250	89.90	2.60	.0819	42.86	5.10	.0292	18.23	7.60	.0144	11.70
.15	.1250	89.79	2.65	.0802	41.86	5.15	.0287	18.02	7.65	.0142	11.61
.20	.1250	89.62	2.70	.0784	40.90	5.20	.0282	17.83	7.70	.0140	11.53
0.25	0.1250	89.40	2.75	0.0767	39.98	5.25	0.0278	17.63	7.75	0.0139	11.45
.30	.1250	89.14	2.80	.0750	39.05	5.30	.0273	17.44	7.80	.0137	11.37
.35	.1250	88.83	2.85	.0731	38.17	5.35	.0269	17.26	7.85	.0136	11.29
.40	.1250	88.47	2.90	.0717	37.32	5.40	.0264	17.08	7.90	.0134	11.21
.45	.1249	88.07	2.95	.0701	36.50	5.45	.0260	16.90	7.95	.0133	11.14
0.50	0.1249	87.61	3.00	0.0685	35.70	5.50	0.0256	16.73	8.00	0.0131	11.06
.55	.1248	87.11	3.05	.0670	34.83	5.55	.0252	16.56	8.05	.0130	10.98
.60	.1248	86.57	3.10	.0655	34.18	5.60	.0248	16.39	8.10	.0128	10.91
.65	.1247	85.97	3.15	.0640	33.46	5.65	.0244	16.23	8.15	.0127	10.84
.70	.1246	85.33	3.20	.0626	32.77	5.70	.0240	16.07	8.20	.0125	10.77
0.75	0.1244	84.65	3.25	0.0612	32.09	5.75	0.0237	15.91	8.25	0.0124	10.70
.80	.1243	83.91	3.30	.0598	31.45	5.80	.0233	15.76	8.30	.0122	10.63
.85	.1240	83.14	3.35	.0585	30.82	5.85	.0230	15.61	8.35	.0121	10.56
.90	.1238	82.32	3.40	.0572	30.22	5.90	.0226	15.46	8.40	.0120	10.49
.95	.1236	81.45	3.45	.0559	29.64	5.95	.0223	15.32	8.45	.0119	10.42
1.00	0.1232	80.55	3.50	0.0547	29.08	6.00	0.0220	15.18	8.50	0.0117	10.36
1.05	.1228	79.60	3.55	.0535	28.53	6.05	.0216	15.04	8.55	.0116	10.29
1.10	.1224	78.61	3.60	.0523	28.01	6.10	.0213	14.90	8.60	.0115	10.22
1.15	.1219	77.59	3.65	.0512	27.51	6.15	.0210	14.77	8.65	.0114	10.16
1.20	.1213	76.53	3.70	.0501	27.02	6.20	.0207	14.63	8.70	.0112	10.10
1.25	0.1207	75.44	3.75	0.0490	26.55	6.25	0.0204	14.50	8.75	0.0111	10.04
1.30	.1200	74.31	3.80	.0480	26.10	6.30	.0201	14.38	8.80	.0110	9.97
1.35	.1193	73.16	3.85	.0470	25.66	6.35	.0199	14.25	8.85	.0109	9.91
1.40	.1185	71.98	3.90	.0460	25.24	6.40	.0196	14.13	8.90	.0108	9.85
1.45	.1176	70.77	3.95	.0451	24.83	6.45	.0193	14.01	8.95	.0107	9.79
1.50	0.1166	69.54	4.00	0.0441	24.43	6.50	0.0191	13.89	9.00	0.0106	9.73
1.55	.1158	68.30	4.05	.0432	24.05	6.55	.0188	13.77	9.05	.0104	9.68
1.60	.1144	67.03	4.10	.0424	23.68	6.60	.0185	13.66	9.10	.0103	9.62
1.65	.1133	65.76	4.15	.0415	23.32	6.65	.0183	13.54	9.15	.0102	9.56
1.70	.1120	64.47	4.20	.0407	22.98	6.70	.0181	13.43	9.20	.0101	9.51
1.75	0.1107	63.18	4.25	0.0399	22.64	6.75	0.0178	13.32	9.25	0.0100	9.45
1.80	.1093	61.89	4.30	.0391	22.32	6.80	.0176	13.21	9.30	.0099	9.40
1.85	.1078	60.59	4.35	.0384	22.00	6.85	.0173	13.11	9.35	.0098	9.34
1.90	.1063	59.30	4.40	.0376	21.70	6.90	.0171	13.00	9.40	.0097	9.29
1.95	.1047	58.02	4.45	.0369	21.40	6.95	.0169	12.90	9.45	.0096	9.24
2.00	0.1031	56.74	4.50	0.0362	21.11	7.00	0.0167	12.80	9.50	0.0096	9.18
2.05	.1015	55.47	4.55	.0355	20.84	7.05	.0165	12.70	9.55	.0095	9.13
2.10	.0998	54.22	4.60	.0349	20.56	7.10	.0163	12.60	9.60	.0094	9.08
2.15	.0980	52.98	4.65	.0342	20.30	7.15	.0161	12.50	9.65	.0093	9.03
2.20	.0963	51.77	4.70	.0336	20.05	7.20	.0159	12.41	9.70	.0092	8.98
2.25	0.0945	50.57	4.75	0.0330	19.80	7.25	0.0157	12.31	9.75	0.0091	8.93
2.30	.0927	49.39	4.80	.0324	19.55	7.30	.0155	12.22	9.80	.0090	8.88
2.35	.0909	48.24	4.85	.0319	19.32	7.35	.0153	12.13	9.85	.0089	8.84
2.40	.0891	47.11	4.90	.0313	19.09	7.40	.0151	12.04	9.90	.0088	8.79
2.45	.0873	46.01	4.95	.0308	18.86	7.45	.0149	11.95	9.95	.0088	8.74
2.50	0.0855	44.93	5.00	0.0302	18.65	7.50	0.0147	11.87	10.00	0.0087	8.69

Fortran IV Program of Womersley's Method

```

SIBFTC MAIN
C   R M ZUMBRUNNEN
C   **** WOMERSLEYS SOLUTION FOR INCOMPRESSIBLE PULSATILE FLOW ****
C   A = COEFFICIENT OF FOURIER SERIES
C   ACC = ACCURACY OF FOURIER REPRESENTATION
C   ALPHA, AL = FREQUENCY PARAMETER
C   AZERO = CONSTANT (MEAN) OF FOURIER SERIES
C   B = COEFFICIENT OF FOURIER SERIES
C   CALCQ = CALCULATED FLOW RATE (CU IN)/SEC
C   DELP = MEASURED PRESSURE GRADIENT (PSI/XFT)
C   DELPF = FOURIER REPRESENTATION OF PRESSURE GRADIENT (PSI/FT)
C   DENS = DENSITY OF FLUID MEDIUM LBS/(CU FT)
C   DOMEGT = INCREMENT BETWEEN DATA POINTS (RADIAN)
C   EPSILN, EP = PHASE ANGLE COMPLEMENT (RADIAN,DEGREE)
C   FMPOAS, FMP = AMPLITUDE FACTOR
C   FMU = DYNAMIC VISCOSITY (LB SEC)/(SQ FT)
C   FREQ = PULSE FREQUENCY (CPS)
C   L = MAXIMUM ALLOWABLE NUMBER OF FOURIER TERMS
C   M = NUMBER OF DATA POINTS
C   OMEGT = ANGLE IN CYCLE (RADIAN)
C   QBAR = MEASURED MEAN FLOW RATE (GPM)
C   RAD = TEST SECTION RADIUS (FT)
C   RHO = DENSITY/GRAVITY SLUGS/(CU FT)
C   RNBAR = REYNOLDS NUMBER FOR EQUIVALENT STEADY FLOW
C   S = STOKES NUMBER OF FIRST HARMONIC
C   TXPQ = EXPERIMENTAL FLOW RATE (CU IN)/SEC
C   XFT = DISTANCE BETWEEN PRESSURE MEASUREMENT LOCATIONS (FT)
C   XPQ = UNCALIBRATED EXPERIMENTAL FLOW RATE (CU UNITS)/SEC
      DIMENSION AL(201),FMP(201),EP(201),A(50),B(50),DELP(100),
1  FMPOAS(50),EPSILN(50), DELPF(50), TXPQ(100), XPQ(100)
      READ 4, (AL(I), I=1,201)
      READ 41,(FMP(I), I=1,201)
      READ 4, (EP(I), I=1,201)
27  READ 2, RAD, FREQ, DENS, FMU, QBAR
      READ 5, XFT, ACC, M, L
      READ 7, (DELP(I), I=1,M)
      READ 7, (XPQ(I), I=1,M)
      DO 19 I = 1,M
19  DELP(I) = DELP(I)/XFT
      TM = M
      DOMEGT = 2.*3.141593/TM
      RHO = DENS/32.174
      S = 8.*3.141593*RAD*RAD*FREQ*RHO/FMU
      ALPHA = RAD*SQRT((6.283184*FREQ*RHO)/FMU)
      RNBAR = 2.*RHO*QBAR/(1410.14*RAD*FMU)
      PRINT 22
      PRINT 99, RAD,FREQ,RHO,DENS,FMU
      PRINT 23
      PRINT 98, QBAR,RNBAR,ALPHA,S
      CALL CLBRTE(M,DOMEGT,XPQ,TXPQ,QBAR,100,FREQ)
      CALL FOURR(DOMEGT,ACC,M,N,DELP,AZERO,A,B,DELPF,L,100,50)
      QZERO = QBAR*231./60.
      DO 15 I=1,N
      FI = I
      ALPHA = RAD*SQRT((6.283184*FI*FREQ*RHO)/FMU)

```

```

      IF (ALPHA-10.) 3,3,6
3  CALL INTRPL(AL, FMP, ALPHA, FMPO)
   CALL INTRPL(AL, EP, ALPHA, EPSI)
   FMPOAS(I) = FMPO
   EPSILN(I) = EPSI/57.2958
   GO TO 15
6  IF (ALPHA-20.) 9, 9, 12
9  FMPOAS(I) = (1.-1.414214/ALPHA+1./(ALPHA*ALPHA))/(ALPHA*ALPHA)
   EPSILN(I) = 1.414214/ALPHA+1./(ALPHA*ALPHA)+.55979/(ALPHA*
1 ALPHA*ALPHA)
   GO TO 15
12 FMPOAS(I) = 1./(ALPHA*ALPHA)
   EPSILN(I) = 0.
15 CONTINUE
   PRINT 81
   DO 100 J=1,M
   FJ = J
   OMEGT = FJ*DOMEGT
   SIGQ = 0.
   DO 80 I = 1,N
   FI = I
80  SIGQ = SIGQ + ((A(I)*SIN(EPSILN(I))-B(I)*COS(EPSILN(I)))
1 *COS(FI*OMEGT) + (A(I)*COS(EPSILN(I)) + B(I)*SIN(EPSILN(I)))
2 *SIN(FI*OMEGT))*3.141593*RAU*RAU*RAU*RAU*FMPOAS(I)/FMU
   CALCQ = QZERO + SIGQ *1728.*144.
   PRINT 82, OMEGT, DELPF(J), DELP(J), CALCQ, TXPQ(J)
100 CONTINUE
   GO TO 27
2  FORMAT(5F15.8)
4  FORMAT(16F5.2)
5  FORMAT(2F15.8, 2I10)
7  FORMAT(8F10.5)
22 FORMAT(75H1          RAD          FREQ          RHO          DENS
1      FMU          )
23 FORMAT(55H0          GRAR          RNBAR          ALPHA          S )
41 FORMAT(16F5.4)
81 FORMAT(75H0          OMEGT          DELPF          DELP          CALCQ
1      TXPQ          )
82 FORMAT(1H , 5F13.6)
98 FORMAT(1H , F13.6, F13.2, F13.6, F13.2)
99 FORMAT(1H , 4F13.6, F13.8)
   END

```

Flow Meter Calibration Subroutine

```
$IBFTC CLBRTE
      SUBROUTINE CLBRTE(M,DOMEGT,XPQ,TXPQ,QBAR,JB,FREQ)
C      R M ZUMBRUNNEN
C      PROGRAM TO CALIBRATE FLOW RATE
      DIMENSION XPQ(JB), TXPQ(JB)
      SUM = 0.
      DT = DOMEGT/(2.*3.141593*FREQ)
      DO 50 I = 1,M
50    SUM = DT*XPQ(I) + SUM
      XBAR = SUM*FREQ
      FACT = QBAR*231./(60.*XBAR)
      DO 60 I = 1,M
60    TXPQ(I) = FACT*XPQ(I)
      RETURN
      END
```

Subroutine for Fourier Representation

```

$IBFTC FOURR
      SUBROUTINE FOURR(DELX,ACC,M,N,Y,AZERO,A,B,PT,L,MM,NN)
C      R M ZUMBRUNNEN
C      PROGRAM TO COMPUTE FOURIER COEFFICIENTS
      1 DIMENSION A(NN), B(NN), Y(MM), PT(MM)
      K = 1
      N = 1
      7 AAZERO = 0.
      8 DO 9 I = 1,M
      9 AAZERO = Y(I) + AAZERO
      10 AZERO = AAZERO*DELX/(2.*3.141593)
      13 DO 20 J = K,N
      131 ANN = 0.
      132 BNN = 0.
      133 FJ = J
      14 DO 18 I = 1,M
      16 FI = I
      17 ANN = Y(I)*COS(FJ*FI*DELX) + ANN
      18 BNN = Y(I)*SIN(FJ*FI*DELX) + BNN
      19 A(J) = DELX*ANN/3.141593
      20 B(J) = DELX*BNN/3.141593
      79 DO 84 I = 1,M
      791 FI = I
      80 PTT = 0.
      81 DO 83 J = 1,N
      82 FJ = J
      83 PTT = A(J)*COS(DELX*FJ*FI) + B(J)*SIN(DELX*FJ*FI) + PTT
      84 PT(I) = AZERO + PTT
      DO 60 I=1,M
      IF(ABS (PT(I)-Y(I))-ACC) 60, 60, 62
      62 IF(N-L ) 63,100, 100
      63 K = N + 1
      N = N + 1
      GO TO 13
      60 CONTINUE
      GO TO 103
      100 PRINT 101
      101 FORMAT(55H0          LIMIT ON NUMBER OF TERMS HIT          )
      103 PRINT 34
      35 PRINT 40, (A(J), J = 1,N)
      37 PRINT 38
      39 PRINT 40, (B(J), J = 1,N)
      34 FORMAT(55H0          -A- COEFFICIENTS FOLLOW, READ ACROSS    )
      38 FORMAT(55H0          -B- COEFFICIENTS FOLLOW, READ ACROSS    )
      40 FORMAT(1H , 5F13.6)
      RETURN
      END
  
```

Linear Interpolation Subroutine

```
SUBFC INTRPL
      SUBROUTINE INTRPL (X, Y, XPT, YPT)
C      R M ZUMBRUNNEN
C      PROGRAM TO PERFORM SIMPLE LINEAR INTERPOLATION
      DIMENSION X(201), Y(201)
      DO 5 J=1,201
      IF(XPT-X(J)) 15, 10, 5
      5 CONTINUE
      10 YPT = Y(J)
      GO TO 20
      15 YPT=Y(J-1) + (Y(J)-Y(J-1))*(XPT-X(J-1))/(ABS(X(J)-X(J-1)))
      20 RETURN
      25 END
```

Sample Computer Output, Run 13

RAD	FREQ	RHO	DENS	FMU
0.018230	1.515000	1.939454	62.400000	0.00002360
QBAR	RNBAR	ALPHA	S	
0.329500	2106.71	16.123771	1039.90	

-A- COEFFICIENTS FOLLOW, READ ACROSS

-0.098771	0.052643	0.000051	0.011715	0.015436
0.011454	0.022062	0.002571	-0.000172	-0.018710
0.025844	-0.042945	0.018362	-0.013272	0.002716
-0.002105				

-B- COEFFICIENTS FOLLOW, READ ACROSS

-0.061601	-0.013390	-0.032335	0.008173	-0.019481
0.012550	-0.009195	0.030602	-0.003501	0.019456
-0.013054	-0.005233	0.024942	-0.021247	0.018849
-0.015861				

OMEGT	DELPH	DELP	CALCQ	TXPQ
0.190400	0.008606	0.008606	2.139467	2.061618
0.380799	-0.141996	-0.141997	1.983629	1.616955
0.571199	-0.215146	-0.215146	1.432075	1.172293
0.761598	-0.131669	-0.131670	0.964844	0.929749
0.951998	-0.075732	-0.075731	0.688827	0.889325
1.142397	-0.101549	-0.101549	0.482959	0.404239
1.332797	-0.135972	-0.135972	0.138378	0.363815
1.523197	-0.086058	-0.086059	-0.157399	0.226374
1.713596	-0.025818	-0.025818	-0.311205	-0.040424
1.903996	-0.030120	-0.030120	-0.359645	-0.161696
2.094395	-0.021515	-0.021515	-0.467236	-0.323391
2.284795	0.028399	0.028399	-0.450314	-0.040424
2.475194	0.079174	0.079174	-0.343736	-0.064678
2.665594	0.077453	0.077453	-0.113584	-0.080848
2.855994	0.094664	0.094664	0.030774	0.080848
3.046393	0.098967	0.098967	0.331172	0.242543
3.236793	0.107573	0.107573	0.433788	0.646782
3.427192	0.447504	0.447504	1.218453	1.293564
3.617592	0.051635	0.051635	1.912585	1.455260
3.807992	0.137694	0.137694	1.927741	1.899923
3.998391	0.172117	0.172117	2.431819	2.263738
4.188791	-0.025818	-0.025818	2.479912	2.304162
4.379190	0.068847	0.068847	2.460061	2.425433
4.569590	0.033563	0.033563	2.556875	2.328416
4.759989	-0.032702	-0.032702	2.467092	2.304162
4.950389	0.025818	0.025818	2.369633	2.263738
5.140788	0.005163	0.005164	2.380316	2.425433
5.331188	-0.006885	-0.006885	2.281528	2.223314
5.521588	0.021515	0.021515	2.266779	2.182890
5.711987	-0.010327	-0.010327	2.224719	2.263738
5.902387	0.002582	0.002582	2.165833	2.021194
6.092786	0.012909	0.012909	2.155209	2.182890
6.283186	0.000000	0.000000	2.141550	2.102042

REFERENCES

1. Grace, S. F.: Oscillatory Motion of a Viscous Liquid in a Long Straight Tube. Philosophical Magazine, Ser. 17, No. 5, 1928, pp. 933-939.
2. McDonald, Donald A.: Blood Flow in Arteries. Baltimore, Maryland. The Williams and Wilkins Company, 1960.
3. Womersley, J. R.: Method for the Calculation of Velocity Rate of Flow, and Viscous Drag in Arteries when the Pressure Gradient is Known. Journal of Applied Physiology, vol. 127, 1955, pp. 553-564.
4. Linford, Robert G. and Ryan, Norman W.: Pulsatile Flow in Rigid Tubes. Journal of Applied Physiology, vol. 20, 1965, pp. 1078-1081.
5. Goldschmied, F. R.: Analytical Investigation of Fluid Amplifier Dynamic Characteristics. NASA CR-244, July 1965.
6. Schlichting, Hermann: Boundary Layer Theory. Fourth edition. New York City, McGraw-Hill Book Company, Inc., 1960, p. 229.
7. Goldschmied, F. R.; Prakouras, A. G.; and Nelson, R. M.: Experimental Investigation of Fluidic and Peristaltic Heart Pumps. AIAA Paper 66-929, AIAA Annual Meeting, Boston, Massachusetts, December 1966.
8. Zumbrunnen, R. M.: Pulsating Flow of Incompressible Fluids. Master of Science thesis, Department of Mechanical Engineering, University of Utah. August 1966.
9. Rudinger, George: Review of Current Mathematic Methods for the Analysis of Blood Flow. Denver, Colorado. Proceedings of the American Society of Mechanical Engineers Biomedical Fluid Mechanics Symposium, pp. 1 - 33, April 25, 1966.
10. Sarpkaya, Turgut: Experimental Determination of the Critical Reynolds Number for Pulsating Poiseuille Flow. American Society of Mechanical Engineers, Paper No. 66-FE-5, 1966.

APPROVAL

AN EXPERIMENTAL STUDY OF PULSATING FLOW OF INCOMPRESSIBLE VISCOUS FLUIDS IN RIGID PIPES IN THE INTERMEDIATE DAMPING RANGE

By

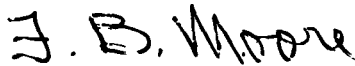
F. R. Goldschmied

The information in this report has been reviewed for security classification. Review of any information concerning Department of Defense or Atomic Energy Commission programs has been made by the MSFC Security Classification Officer. This report, in its entirety, has been determined to be unclassified.

This document has also been reviewed and approved for technical accuracy.


J. BRIDGES

Chief, Flight Control Development Branch



F. R. MOORE

Chief, Guidance and Control Division



W. HAEUSSERMANN

Director, Astrionics Laboratory

DISTRIBUTION

INTERNAL

R-ASTR-DIR

Dr. Haeussermann/Ref. File
Miss Flowers

Professor Fabio R. Goldschmied (50)
Department of Mechanical Engineering
University of Utah
Salt Lake City, Utah 84112

R-ASTR-N

Mr. Moore
Mr. Gassaway
Mr. Kalange (25)
Mr. Tutt
Mr. Wojtalik
Mr. Wood
Mr. Caudle
Mr. Howard
Mr. Cornelius
Record Copy

NASA Headquarters
Office of University Affairs (10)
Code Y
Washington, D. C.

NASA Headquarters
Attn: R. Bohling, REC
Washington, D. C. 20546

PAT

NASA
Langley Research Center
Stability and Controls Section
Attn: P. Kurzhals
Langley Station, Va. 23365

MS-H

MS-IP

NASA
Langley Station
Attn: Douglas H. Garner, MS 494
Hampton, Va. 23365

MS-IL (8)

I-RM-M

MS-T (5)

NASA
Lewis Research Center
Attn: Vernon D. Gebben
Mail Stop 54-4
Cleveland, Ohio 44135

R-P&VE-P

Mr. Paul (2)

EXTERNAL

Scientific and Technical Information
Facility (2)
Attn: NASA Representative (S-AK/RKT)
P. O. Box 33
College Park, Md. 20740

DISTRIBUTION (Concluded)

EXTERNAL (Cont'd)

NASA
Lewis Research Center
Attn: William S. Griffin
Mail Stop 54-4
Cleveland, Ohio 44135

NASA Headquarters
Attn: Carl Janow, Code RED
Washington, D. C. 20546

Harry Diamond Laboratories
Attn: Joseph M. Kirshner, Branch 310
Washington, D. C. 20438

NASA
Electronic Research Center
575 Technology Square
Attn: Dennis Collins
Cambridge, Mass. 02139